

Article

# Structures and Fluorescent and Magnetic Behaviors of Newly Synthesized Ni<sup>II</sup> and Cu<sup>II</sup> Coordination Compounds

Lin-Wei Zhang, Xiao-Yan Li, Quan-Peng Kang, Ling-Zhi Liu, Jian-Chun Ma and Wen-Kui Dong \* 

School of Chemical and Biological Engineering, Lanzhou Jiaotong University, Lanzhou 730070, China; zhanglinwei@mail.lzjtu.cn (L.-W.Z.); L1401569787@163.com (X.-Y.L.); KQpeng2580@163.com (Q.-P.K.); llz1009663202@126.com (L.-Z.L.); majc0204@126.com (J.-C.M.)

\* Correspondence: dongwk@126.com; Tel.: +86-931-4938-703

Received: 20 March 2018; Accepted: 16 April 2018; Published: 18 April 2018



**Abstract:** Newly designed three trinuclear coordination compounds  $[\text{Ni}_3(\text{L}^1)_2(\text{OAc})_2(\text{CH}_3\text{OH})_2]$  (**1**),  $[\text{Ni}_3(\text{L}^1)_2(\text{OAc})_2(\text{CH}_3\text{CH}_2\text{CH}_2\text{OH})_2] \cdot 2\text{CH}_3\text{CH}_2\text{CH}_2\text{OH}$  (**2**) and  $[\text{Ni}_3(\text{L}^1)_2(\text{OAc})_2(\text{DMF})_2] \cdot 1.71\text{DMF}$  (**3**) and one mononuclear coordination compound  $[\text{Cu}(\text{L}^2)_2]$  (**4**) have been synthesized by  $\text{H}_2\text{L}^1$  and nickel(II) and copper(II) acetate hydrates in different solvents. Single-crystal X-ray structure determinations revealed that the coordination compounds **1–3** have analogous molecular structures. The coordination compounds **1**, **2**, and **3** were affected by the coordinated methanol, *n*-propanol, and *N,N*-dimethylformamide molecules, respectively, and the various coordinated solvent molecules give rise to the formation of the representative solvent-induced Ni<sup>II</sup> coordination compounds. All the Ni<sup>II</sup> atoms are six-coordinated with geometries of slightly distorted octahedron. Obviously, in the coordination compound **4**, the expected salamo-like mono- or tri-nuclear Cu<sup>II</sup> coordination compound has not been obtained, but a new Cu<sup>II</sup> coordination compound  $[\text{Cu}(\text{L}^2)_2]$  has been gained. The Cu<sup>II</sup> atom is four-coordinated and possesses a geometry of slightly distorted planar quadrilateral. Furthermore, the fluorescence properties of coordination compounds **1–4** and magnetic behavior of coordination compound **1** were investigated.

**Keywords:** salamo-like ligand; coordination compound; synthesis; crystal structure; property

## 1. Introduction

Salen-like ligands and their analogues continue to play an increasingly vital roles in inorganic chemistry in the last decades [1–4], since their metallic coordination compounds are widely used in catalysis activities [5,6], magnetic materials [7–10], biological fields [11–17], supramolecular architectures [18–21], molecular recognitions [22–25], and luminescence properties [26–30]. It is significant to find appropriate substituted groups for the moieties of the ligands to enhance the properties of these metallic coordination compounds [31–33]. Lately, a number of Salen-like compounds [34–39] (Salamo and its derivatives) has been exploited using *O*-alkyloxime units ( $-\text{CH}=\text{N}-\text{O}-(\text{CH}_2)_n-\text{O}-\text{N}=\text{CH}-$ ) rather than the non *O*-alkyloxime ( $-\text{CH}=\text{N}-(\text{CH}_2)_n-\text{N}=\text{CH}-$ ) units, and the larger electronegativity of oxygen atoms is desired to strongly influence the electronic behavior of the  $\text{N}_2\text{O}_2$  coordination environment, which can give rise to novel structures and different properties of the resulting coordination compounds [40–47]. In addition, metallic ions play important roles in different biological processes and the interaction of the metallic ion with drugs employed for therapeutic reasons [48].

Herein, following our previous research on the syntheses, crystal structures, and fluorescent and antimicrobial properties of Co<sup>II</sup> and Ni<sup>II</sup> coordination compounds with salamo-like bisoxime

ligand  $H_2L^1$  (4,4'-dichloro-2,2'-[(propane-1,3-diylidyoxy)bis(nitrilomethylidyne)]diphenol) [49,50], the alkoxy chain is increasing from two to three on the ligand  $H_2L^1$ , which can give rise to better flexibility and coordination ability. In this paper, four new tri- and mono-nuclear salamo-like  $Ni^{II}$  and  $Cu^{II}$  coordination compounds,  $[Ni_3(L^1)_2(OAc)_2(CH_3OH)_2]$  (**1**),  $[Ni_3(L^1)_2(OAc)_2(CH_3CH_2CH_2OH)_2] \cdot 2CH_3CH_2CH_2OH$  (**2**) and  $[Ni_3(L^1)_2(OAc)_2(DMF)_2] \cdot 1.71DMF$  (**3**) and  $[Cu(L^2)_2]$  (**4**), have been synthesized. X-ray crystal structures revealed that the coordination compounds **1–3** have analogous molecular structures. The coordination compounds **1**, **2**, and **3** were affected by the coordinated methanol, n-propanol, and *N,N*-dimethylformamide molecules, respectively. In the coordination compound **4**, the expected mono- or tri-nuclear salamo-like  $Cu^{II}$  coordination compound has not been gained, but a new  $Cu^{II}$  coordination compound  $[Cu(L^2)_2]$  has been obtained. Moreover, the fluorescent and magnetic behaviors have been discussed.

## 2. Experimental Section

### 2.1. Materials and Methods

5-Chlorosalicylaldehyde (98%) was obtained from Alfa Aesar and used without further purification. 1,3-Dibromopropane and other reagents and solvents were analytical grade reagents from Tianjin Chemical Reagent Factory (Tianjin, China).

C, H, and N analyses were performed using a GmbH VariuoEL V3.00 automatic elemental analysis instrument (Elementar, Berlin, Germany). Elemental analyses for  $Ni^{II}$  or  $Cu^{II}$  were measured with an IRIS ER/S-WP-1 ICP atomic emission spectrometer (Elementar, Berlin, Germany). Melting points were gained via a  $X_4$  microscopic melting point apparatus made by Beijing Taike Instrument Company Limited and were uncorrected. IR spectra were measured on a Vertex 70 FT-IR spectrophotometer (Bruker, Billerica, MA, USA), with samples prepared as KBr (400–4000  $cm^{-1}$ ) pellets. UV-vis absorption spectra were measured on a Shimadzu UV-3900 spectrometer (Shimadzu, Tokyo, Japan).  $^1H$  NMR spectra were performed by German Bruker AVANCE DRX-400/600 spectroscopy (Bruker AVANCE, Billerica, MA, USA). X-ray single crystal structure determinations for the coordination compounds **1**, **2**, **3**, and **4** were carried out on a Bruker Smart Apex CCD and SuperNova, Dual, Cu at zero, Eos four-circle diffractometers. Magnetic susceptibility data were collected on the powdered samples of the coordination compound **1** using a Quantum Design (San Diego, CA, USA) model MPMS XL7 SQUID magnetometer. Magnetic susceptibility measurements were performed at 1000 Oe in the 2–300 K temperature range.

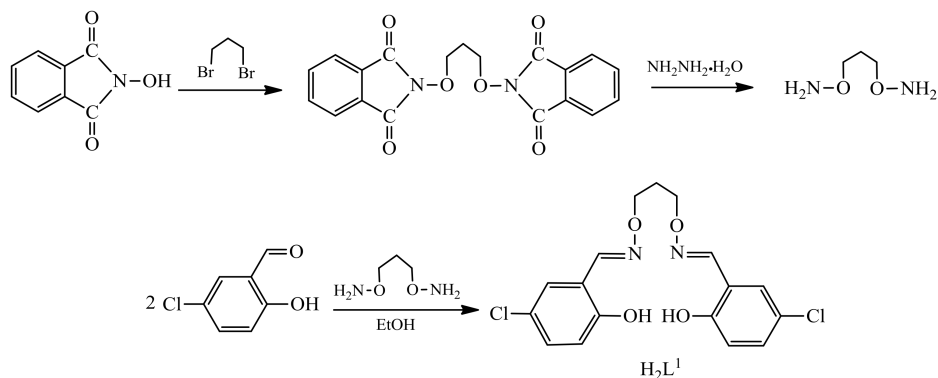
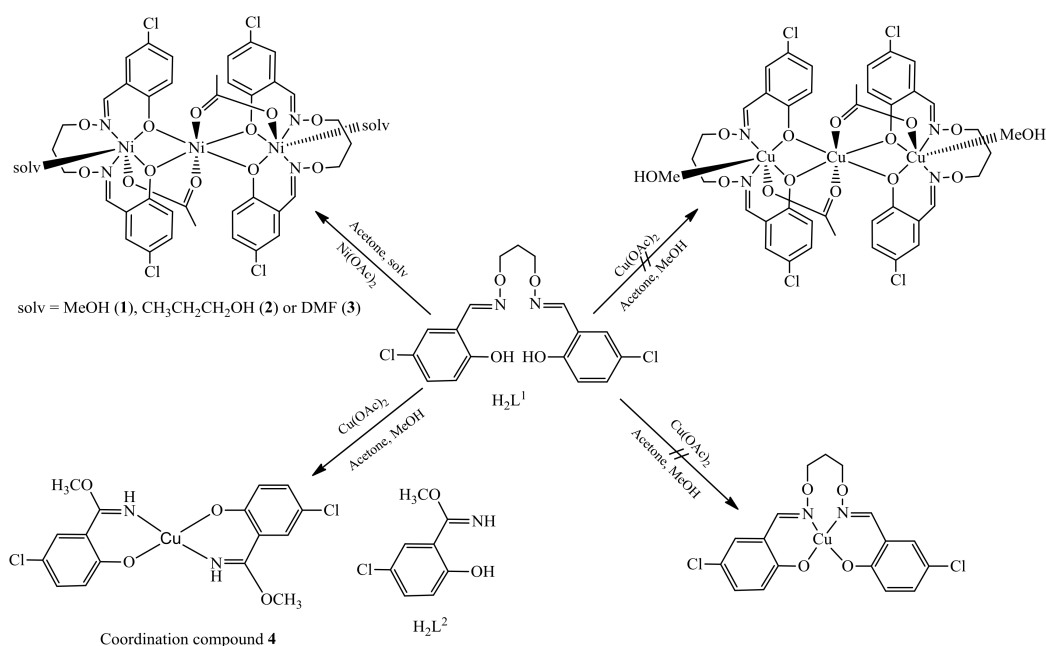
### 2.2. Synthesis of $H_2L^1$

The ligand  $H_2L^1$  was synthesized according to a same method reported earlier [49–51]. (Scheme 1) Yield: 75.8%. m.p. 164–166 °C. Anal. Calcd. for  $C_{17}H_{16}Cl_2N_2O_4$  (%): C, 53.02; H, 4.11; N, 7.45. Found: C, 53.28; H, 4.21; N, 7.31.  $^1H$  NMR (400 MHz,  $CDCl_3$ ),  $\delta$  2.14 (t,  $J = 6.0$  Hz, 2H,  $CH_2$ ), 4.31 (t,  $J = 6.0$  Hz, 4H,  $CH_2$ ), 6.85 (d,  $J = 8.0$  Hz, 2H, ArH), 7.25 (s, 2H, ArH), 7.33 (d,  $J = 8.0$  Hz, 2H, ArH), 8.09 (s, 2H,  $CH=N$ ), 9.80 (s, 2H, OH). IR (KBr,  $cm^{-1}$ ): 3101 [ $\nu(O-H)$ ], 1606 [ $\nu(C=N)$ ], 1263 [ $\nu(Ar-O)$ ]. UV-Vis ( $CHCl_3$ ),  $\lambda_{max}$  (nm) ( $\epsilon_{max}$ ): 223, 267 and 325 nm ( $2.5 \times 10^{-5}$  M).

### 2.3. Syntheses of the Coordination Compounds **1–4**

Tri- and mono-nuclear coordination compounds **1–4** were synthesized by the reaction of  $H_2L^1$  with  $Ni(OAc)_2 \cdot 4H_2O$  and  $Cu(OAc)_2 \cdot 4H_2O$ , respectively (Scheme 2).

A methanol solution (2 mL) of  $Ni(OAc)_2 \cdot 4H_2O$  (5.07 mg, 0.015 mmol) was added dropwise to  $H_2L^1$  (3.83 mg, 0.010 mmol) in acetone (2 mL) and stirred for 30 min. The mixture was filtered, and the filtrate was allowed to stand at room temperature for ca. four weeks on slow evaporation of the solution in the dark. Several green block-like single crystals suitable for X-ray crystallographic analysis were collected and then filtrated and washed with n-hexane. The coordination compounds **2**, **3**, and **4** were prepared by an analogous procedure as for the coordination compound **1**.

Scheme 1. Synthetic route to  $H_2L^1$ .

Scheme 2. Synthetic routes to the coordination compounds 1–4.

Coordination compound **1**, light green crystals. Yield, 2.93 mg (52.3%). Anal. Calcd. for  $C_{40}H_{42}Cl_4Ni_3N_4O_{14}$  (%): C, 42.87; H, 3.78; N, 5.00; Ni, 15.71. Found: C, 43.02; H, 3.82; N, 4.87; Ni, 15.79. IR (KBr,  $cm^{-1}$ ): 3230 [ $\nu(O-H)$ ], 1612 [ $\nu(C=N)$ ], 1197 [ $\nu(Ar-O)$ ]. UV–Vis ( $CHCl_3$ ),  $\lambda_{max}$  (nm) ( $\epsilon_{max}$ ): 234 and 367 nm ( $2.5 \times 10^{-5}$  M).

Coordination compound **2**, light green crystals. Yield, 3.13 mg (48.3%). Anal. Calcd. for  $C_{50}H_{66}Cl_4Ni_3N_4O_{16}$  (%): C, 46.30; H, 5.13; N, 4.32; Ni, 13.58. Found: C, 46.42; H, 5.19; N, 4.26; Ni, 13.63. IR (KBr,  $cm^{-1}$ ): 3354 [ $\nu(O-H)$ ], 1616 [ $\nu(C=N)$ ], 1195 [ $\nu(Ar-O)$ ]. UV–Vis ( $CHCl_3$ ),  $\lambda_{max}$  (nm) ( $\epsilon_{max}$ ): 234 and 365 nm ( $2.5 \times 10^{-5}$  M).

Coordination compound **3**, light green crystals. Yield, 3.96 mg (58.7%). Anal. Calcd. for  $C_{49.12}H_{59.94}Cl_4Ni_3N_{7.71}O_{15.71}$  (%): C, 44.44; H, 4.55; N, 8.13; Ni, 13.26. Found: C, 44.69; H, 4.71; N, 8.16; Ni, 12.88. IR (KBr,  $cm^{-1}$ ): 1629 [ $\nu(C=N)$ ], 1197 [ $\nu(Ar-O)$ ]. UV–Vis ( $CHCl_3$ ),  $\lambda_{max}$  (nm) ( $\epsilon_{max}$ ): 233 and 367 nm ( $2.5 \times 10^{-5}$  M).

Coordination compound **4**, dark green crystals. Yield, 2.82 mg (65.1%). Anal. Calcd. for  $C_{16}H_{14}Cl_2CuN_2O_4$  (%): C, 44.41; H, 3.26; N, 6.47; Cu, 14.68. Found: C, 44.47; H, 3.33; N, 6.34; Cu, 14.73. IR (KBr,  $cm^{-1}$ ): 1623 [ $\nu(C=N)$ ], 1198 [ $\nu(Ar-O)$ ]. UV–Vis ( $CHCl_3$ ),  $\lambda_{max}$  (nm) ( $\epsilon_{max}$ ): 232 and 345 nm ( $2.5 \times 10^{-5}$  M).

#### 2.4. Crystal Structure Determinations of the Coordination Compounds 1–4

The crystal diffractometers with a monochromatic beam of Mo  $K\alpha$  radiation ( $\lambda = 0.71073 \text{ \AA}$ ) produced using Graphite monochromator from a sealed Mo X-ray tube was used for gaining crystal data for the coordination compounds 1–4 at 293(2), 294.39(10) 294.29(10), and 293(2) K, respectively. The program(s) used to solve structure were SHELXS-2008 (Sheldrick, 2008) [52]; the program(s) used to refine structure were SHELXL-2008 (Sheldrick, 2008) [53]. The crystal data and experimental parameters relevant to the structure determinations are listed in Table 1. Supplementary crystallographic data for this paper have been deposited at Cambridge Crystallographic Data Centre (1588647, 1588644, 1588646, and 1588645 for the coordination compounds 1, 2, 3, and 4) and can be obtained free of charge via [www.ccdc.cam.ac.uk/conts/retrieving.html](http://www.ccdc.cam.ac.uk/conts/retrieving.html).

**Table 1.** X-ray crystallographic data for the coordination compounds 1–4.

Coordination Compound	1	2	3	4
Empirical formula	$C_{40}H_{42}Cl_4Ni_3N_4O_{14}$	$C_{50}H_{66}Cl_4Ni_3N_4O_{16}$	$C_{49.12}H_{59.94}Cl_4Ni_3N_{7.71}O_{15.71}$	$C_{16}H_{14}Cl_2CuN_2O_4$
Formula weight	1120.70	1297.00	1327.65	432.73
T (K)	293 (2)	294.39 (10)	293 (2)	293 (2)
Wavelength ( $\text{\AA}$ )	0.71073	0.71073	0.71073	0.71073
Crystal system	triclinic	triclinic	triclinic	monoclinic
Space group	$P - 1$	$P - 1$	$P - 1$	$C 2/c$
$a$ ( $\text{\AA}$ )	9.289 (8)	9.4955 (7)	11.3008 (8)	23.652 (3)
$b$ ( $\text{\AA}$ )	11.630 (10)	12.1979 (7)	11.3069 (10)	5.0493 (6)
$c$ ( $\text{\AA}$ )	14.042 (12)	13.4593 (9)	12.1027 (10)	13.7190 (17)
$\alpha$ ( $^\circ$ )	67.599 (10)	70.556 (6)	102.513 (7)	90
$\beta$ ( $^\circ$ )	76.686 (10)	81.564 (6)	100.115 (7)	95.195 (12)
$\gamma$ ( $^\circ$ )	87.161 (12)	82.607 (6)	94.689 (7)	90
$V$ ( $\text{\AA}^3$ )	1364 (2)	1448.76 (17)	1474.7 (2)	1631.7 (3)
$Z$	1	1	1	4
$D_{\text{calc}}$ ( $\text{g}\cdot\text{cm}^{-3}$ )	1.365	1.487	1.495	1.762
Absorption coefficient ( $\text{mm}^{-1}$ )	1.279	1.217	1.199	1.691
$F(000)$	574	674	686	876
Crystal size (mm)	$0.19 \times 0.22 \times 0.26$	$0.24 \times 0.25 \times 0.29$	$0.17 \times 0.24 \times 0.26$	$0.04 \times 0.05 \times 0.37$
$\theta$ Range ( $^\circ$ )	1.611–26.492	3.40–26.02	3.519–26.020	3.31–26.02
	$-11 \leq h \leq 11$	$-11 \leq h \leq 11$	$-13 \leq h \leq 13$	$-23 \leq h \leq 28$
Index ranges	$-14 \leq k \leq 13$	$-15 \leq k \leq 14$	$-13 \leq k \leq 13$	$-6 \leq k \leq 3$
	$-17 \leq l \leq 17$	$-16 \leq l \leq 16$	$-14 \leq l \leq 14$	$-12 \leq l \leq 16$
Reflections collected/unique	10,579/5502	9926/5688	10,346/5788	3049/1608
	[ $R_{\text{int}} = 0.0713$ ]	[ $R_{\text{int}} = 0.0369$ ]	[ $R_{\text{int}} = 0.0374$ ]	[ $R_{\text{int}} = 0.0259$ ]
Completeness to $\theta$	97.7% ( $\theta = 25.24$ )	99.8% ( $\theta = 26.00$ )	99.8% ( $\theta = 25.242$ )	99.9% ( $\theta = 25.50$ )
Data/restraints/parameters	5502/0/297	5688/3/359	5788/36/373	1608/0/120
GOF	1.041	1.038	1.053	1.061
Final $R_1$ , $wR_2$ indices	0.0747, 0.1880	0.0492, 0.1081	0.0524, 0.1188	0.0376, 0.0833
$R_1$ , $wR_2$ indices (all data)	0.1330, 0.2102	0.0721, 0.1239	0.0821, 0.1422	0.0517, 0.0948

### 3. Results and Discussion

#### 3.1. IR Spectra

The FT-IR spectral results of  $H_2L^1$  and its corresponding coordination compounds 1–4 exhibited different bands in the  $4000\text{--}400 \text{ cm}^{-1}$  region (Figure 1).

A typical C=N stretching band of  $H_2L^1$  appeared at  $1606 \text{ cm}^{-1}$ , and that of the coordination compounds 1–4 appeared at 1612, 1616, 1629, and  $1623 \text{ cm}^{-1}$ , respectively [54,55]. The C=N stretching bands are shifted to high wavenumber, exhibiting that the  $Ni^{II}$  and  $Cu^{II}$  atoms are bonded by oxime nitrogen atoms of deprotonated  $(L^2)^{2-}$  and  $(L^1)^-$  moieties. Hence, conclusion could be given that the ligands  $H_2L^1$  and  $H_2L^2$  have bonded with  $Ni^{II}$  and  $Cu^{II}$  atoms [56,57]. The free ligand  $H_2L^1$  exhibited a Ar–O stretching band at  $1263 \text{ cm}^{-1}$ , while the Ar–O stretching bands of the coordination compounds 1–4 appeared at 1197, 1195, 1197, and  $1198 \text{ cm}^{-1}$ , respectively. The Ar–O stretching bands are waved to low wavenumber, which could be presence of the coordination of phenolic oxygen to  $Ni^{II}$  and  $Cu^{II}$  atoms [58,59]. The free ligand  $H_2L^1$  showed a desired absorption band at  $3101 \text{ cm}^{-1}$ , which as an evidence for the presence of phenolic OH groups. The expected OH stretching absorption bands in the coordination compounds 1 and 2 are observed at  $3230$  and  $3354 \text{ cm}^{-1}$ , exhibiting the existence

of coordinated methanol and n-propanol molecules, respectively [60]. Furthermore, a N–H stretching band is observed at  $3353\text{ cm}^{-1}$  in the coordination compound 4.

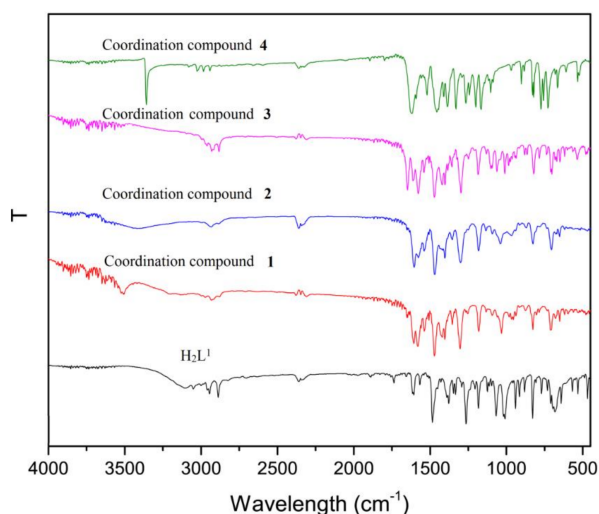


**Figure 1.** Infrared spectra of  $\text{H}_2\text{L}^1$  and its coordination compounds 1–4.

### 3.2. UV-vis Absorption Spectra

UV-vis absorption spectral results of  $\text{H}_2\text{L}^1$  and its coordination compounds 1–4 were determined in  $2.5 \times 10^{-5}\text{ M}$  chloroform solution and are shown in Figure 2.

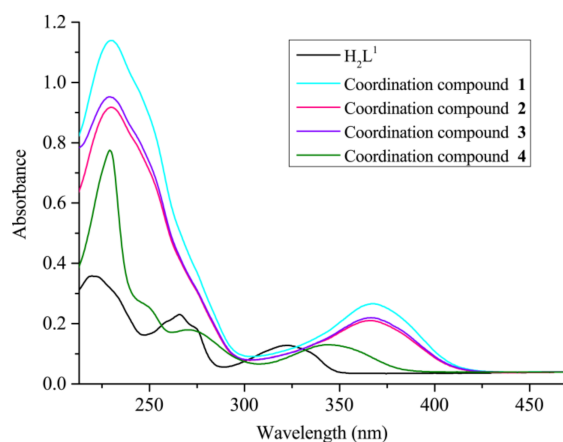


**Figure 2.** UV-vis spectra of  $\text{H}_2\text{L}^1$  and its coordination compounds 1–4 in chloroform ( $c = 2.5 \times 10^{-5}\text{ M}$ ).

The absorption spectrum of  $\text{H}_2\text{L}^1$  showed three absorption peaks at ca. 223, 267, and 325 nm, the peaks at 223 and 267 nm can be assigned to the  $\pi\text{-}\pi^*$  transitions of the phenyl rings, and the peak at 325 nm can be attributed to the  $\pi\text{-}\pi^*$  transitions of the oxime group [61,62]. Compared to  $\text{H}_2\text{L}^1$ , with the appearance of the first peaks at about 233 nm are observed in the coordination compounds 1–4, These absorption peaks are shifted bathochromically, exhibiting coordination of the  $(\text{L}^1)^{2-}$  and  $(\text{L}^2)^-$  moieties with  $\text{Ni}^{\text{II}}$  and  $\text{Cu}^{\text{II}}$  atoms. The absorption peak at ca. 267 nm is absent in the coordination compounds 1–4. Meanwhile, new absorption peaks are observed at about 345–367 nm in the coordination compounds 1–4 that might be owing to  $\text{L}\rightarrow\text{M}$  charge-transfer transitions, which are characteristic of the transition metallic coordination compounds with  $\text{N}_2\text{O}_2$  coordination spheres [63–65].

## 3.3. Descriptions of the Crystal Structures

Selected bond lengths and angles for the coordination compounds 1–3 and 4 are presented in Tables 2 and 3, respectively. The relative hydrogen bonds of the coordination compounds 1–4 are listed in Table 4.

**Table 2.** Selected bond lengths (Å) and angles (°) for the coordination compounds 1–3.

Coordination Compound 1		Coordination Compound 2		Coordination Compound 3	
Bond	Lengths	Bond	Lengths	Bond	Lengths
Ni1-O3	2.012(4)	Ni1-O1	2.019(2)	Ni1-O1	2.085(3)
Ni1-O4	2.021(4)	Ni1-O4	2.023(2)	Ni1-O4	2.106(2)
Ni1-O5	2.099(5)	Ni1-O5	2.035(2)	Ni1-O6	2.033(3)
Ni1-O6	2.029(5)	Ni1-O6	2.112(3)	Ni1-O1 <sup>#3</sup>	2.085(3)
Ni1-N1	2.088(5)	Ni1-N1	2.057(3)	Ni1-O4 <sup>#3</sup>	2.106(2)
Ni1-N2	2.074(5)	Ni1-N2	2.057(3)	Ni1-O6 <sup>#3</sup>	2.032(3)
Ni2-O3	2.067(4)	Ni2-O1	2.071(2)	Ni2-O1	2.032(2)
Ni2-O3 <sup>#1</sup>	2.067(4)	Ni2-O1 <sup>#2</sup>	2.071(2)	Ni2-O4	2.032(3)
Ni2-O4	2.041(4)	Ni2-O4	2.080(2)	Ni2-O5	2.023(3)
Ni2-O4 <sup>#1</sup>	2.041(4)	Ni2-O4 <sup>#2</sup>	2.080(2)	Ni2-O7	2.167(3)
Ni2-O7	2.072(5)	Ni2-O8	2.084(2)	Ni2-N1	2.053(3)
Ni2-O7 <sup>#1</sup>	2.072(5)	Ni2-O8 <sup>#2</sup>	2.084(2)	Ni2-N2	2.072(4)
Bond	Angles	Bond	Angles	Bond	Angles
O3-Ni1-O4	78.32(15)	O1-Ni1-O4	79.68(10)	O1-Ni1-O4	79.36(10)
O3-Ni1-O5	90.92(17)	O1-Ni1-O5	91.06(10)	O1-Ni1-O1 <sup>#3</sup>	180.0
O3-Ni1-O6	91.44(17)	O1-Ni1-O6	91.24(10)	O1-Ni1-O4 <sup>#3</sup>	100.64(10)
O3-Ni1-N1	86.93(16)	O1-Ni1-N1	87.83(11)	O6-Ni1-O1	87.39(11)
O3-Ni1-N2	163.80(17)	O1-Ni1-N2	167.87(11)	O6-Ni1-O4	90.14(11)
O4-Ni1-O5	89.55(19)	O4-Ni1-O5	93.90(10)	O6-Ni1-O4 <sup>#3</sup>	89.86(11)
O4-Ni1-O6	95.26(18)	O4-Ni1-O6	88.25(11)	O6-Ni1-O1 <sup>#3</sup>	92.62(11)
O4-Ni1-N1	164.23(18)	O4-Ni1-N1	166.63(11)	O6-Ni1-O6 <sup>#3</sup>	180.0
O4-Ni1-N2	85.86(17)	O4-Ni1-N2	88.34(11)	O1 <sup>#3</sup> -Ni1-O4 <sup>#3</sup>	79.36(10)
O5-Ni1-O6	174.98(16)	O5-Ni1-O6	177.10(10)	O1 <sup>#3</sup> -Ni1-O4	100.64(10)
O5-Ni1-N1	85.1(2)	O5-Ni1-N1	91.04(11)	O4 <sup>#3</sup> -Ni1-O4	180.0
O5-Ni1-N2	92.4(2)	O5-Ni1-N2	91.68(11)	O6 <sup>#3</sup> -Ni1-O4 <sup>#3</sup>	90.14(11)
O6-Ni1-N1	90.6(2)	O6-Ni1-N1	87.28(13)	O6 <sup>#3</sup> -Ni1-O1 <sup>#3</sup>	92.62(11)
O6-Ni1-N2	86.5(2)	O6-Ni1-N2	86.43(12)	O6 <sup>#3</sup> -Ni1-O1	92.61(11)
N1-Ni1-N2	109.15(18)	N1-Ni1-N2	103.93(12)	O6 <sup>#3</sup> -Ni1-O4	89.86(11)
O3-Ni2-O3 <sup>#1</sup>	180.0	O1-Ni2-O1 <sup>#2</sup>	180.0	O1-Ni2-O7	90.12(11)
O3-Ni2-O4	76.62(15)	O1-Ni2-O4	77.20(9)	O1-Ni2-N1	169.59(12)
O3-Ni2-O4 <sup>#1</sup>	103.38(15)	O1-Ni2-O4 <sup>#2</sup>	102.80(9)	O1-Ni2-N2	86.70(12)
O3-Ni2-O7	90.29(17)	O1-Ni2-O8	90.11(9)	O4-Ni2-N1	88.32(12)
O3-Ni2-O7 <sup>#1</sup>	89.71(17)	O1-Ni2-O8 <sup>#2</sup>	89.89(9)	O4-Ni2-N2	169.28(12)
O3 <sup>#1</sup> -Ni2-O4	103.38(15)	O1 <sup>#2</sup> -Ni2-O4	102.80(9)	O4-Ni2-O1	82.93(11)
O3 <sup>#1</sup> -Ni2-O4 <sup>#1</sup>	76.62(15)	O1 <sup>#2</sup> -Ni2-O4 <sup>#2</sup>	77.20(9)	O4-Ni2-O5	90.72(11)
O3 <sup>#1</sup> -Ni2-O7	89.71(17)	O1 <sup>#2</sup> -Ni2-O8	89.89(9)	O4-Ni2-O7	92.00(11)
O3 <sup>#1</sup> -Ni2-O7 <sup>#1</sup>	90.29(17)	O1 <sup>#2</sup> -Ni2-O8 <sup>#2</sup>	90.11(9)	O5-Ni2-O1	91.71(11)
O4-Ni2-O4 <sup>#1</sup>	180.0	O4-Ni2-O4 <sup>#2</sup>	180.00(13)	O5-Ni2-O7	176.89(11)
O4-Ni2-O7	88.39(16)	O4-Ni2-O8	89.72(9)	O5-Ni2-N1	94.04(12)
O4-Ni2-O7 <sup>#1</sup>	91.61(16)	O4-Ni2-O8 <sup>#2</sup>	90.28(9)	O5-Ni2-N2	92.32(13)
O4 <sup>#1</sup> -Ni2-O7	91.61(16)	O4 <sup>#2</sup> -Ni2-O8	90.28(9)	N1-Ni2-O7	84.54(12)
O4 <sup>#1</sup> -Ni2-O7 <sup>#1</sup>	88.39(16)	O4 <sup>#2</sup> -Ni2-O8 <sup>#2</sup>	89.72(9)	N1-Ni2-N2	101.71(13)
O7-Ni2-O7 <sup>#1</sup>	180.0(2)	O8-Ni2-O8 <sup>#2</sup>	180.0	N2-Ni2-O7	85.27(13)

Symmetry transformations used to generate equivalent atoms: <sup>#1</sup>  $-x + 1, -y + 1, -z + 1$ ; <sup>#2</sup>  $x + 1, y + 1, z$ ; <sup>#3</sup>  $-x, -y, -z + 1$ .

**Table 3.** Selected bond lengths (Å) and angles (°) for the coordination compound 4.

Bond	Lengths	Bond	Lengths
Cu1-O1	1.910(2)	Cu1-O1 <sup>#4</sup>	1.910(2)
Cu1-N1	1.915(3)	Cu1-N1 <sup>#4</sup>	1.915(3)
Bond	Angles	Bond	Angles
O1-Cu1-O1 <sup>#4</sup>	180.0	O1-Cu1-N1	87.92(11)
O1-Cu1-N1 <sup>#4</sup>	92.08(11)	O1 <sup>#4</sup> -Cu1-N1	92.08(11)
O1 <sup>#4</sup> -Cu1-N1 <sup>#4</sup>	87.93(11)	N1-Cu1-N1 <sup>#4</sup>	180.0

Symmetry transformations used to generate equivalent atoms: <sup>#4</sup> -x, -y, -z + 1.**Table 4.** Hydrogen bonding interactions [Å °] for the coordination compounds 1–4.

D-H...A	d(D-H)	d(H-A)	d(D-A)	∠D-X-A
Coordination compound 1				
O5-H5...O3	0.87	2.57	2.932(7)	106
C3-H3...O7	0.93	2.53	3.238(7)	133
C8-H8B...O2	0.97	2.44	2.810(8)	102
C10-H10B...O1	0.97	2.56	2.888(9)	100
C10-H10B...O6	0.97	2.48	3.381(10)	154
C16-H16...O7	0.93	2.58	3.234(8)	128
Coordination compound 2				
O6-H6...O7	0.86(4)	1.78(4)	2.637(5)	174(2)
O7-H7A...O8	0.70(5)	2.08(5)	2.777(4)	171(5)
C8-H8A...O5	0.97	2.55	3.380(6)	143
Coordination compound 3				
C8-H8A...O5	0.97	2.38	3.226(6)	146
C10-H10B...O5	0.97	2.55	3.340(5)	138
C20-H20...O6	0.93	2.45	3.360(5)	167
C22-H22C...O7	0.96	2.42	2.752(8)	100
C24-H24B...O8	0.96	2.15	2.543(17)	103
C13-H13...O8	0.93	2.48	3.306(10)	149
C25-H25B...O3	0.96	2.48	3.418(13)	165
C23-H23...O8	0.93	2.60	3.328(16)	139
Coordination compound 4				
N1-H1...O1	0.70(4)	2.45(3)	2.655(4)	100(3)
C5-H5...O2	0.93	2.28	2.633(4)	102

### 3.3.1. Crystal Structures of the Coordination Compounds 1–3

The coordination compound **1** belongs to the triclinic system, with space group  $P - 1$ , which includes of three Ni<sup>II</sup> atoms, two completely deprotonated (L<sup>1</sup>)<sup>2-</sup> units, two  $\mu_2$ -acetato ligands, and two coordinated methanol molecules. The terminal Ni<sup>II</sup> atoms (Ni1 or Ni1 <sup>#1</sup>) are six-coordinated by two oxime nitrogen atoms (N1, N2 or N1 <sup>#1</sup>, N2 <sup>#1</sup>) and two phenoxo oxygen atoms (O5, O6 or O5 <sup>#1</sup>, O6 <sup>#1</sup>), the four atoms mentioned above are all from one deprotonated (L<sup>1</sup>)<sup>2-</sup> units, one oxygen atom (O4 or O4 <sup>#1</sup>) from the  $\mu_2$ -acetato ligands and one oxygen atom (O7 or O7 <sup>#1</sup>) from the coordinated methanol molecules (Figure 3). The central Ni<sup>II</sup> atom (Ni2) is also six-coordinated via four phenoxo oxygen atoms from two (L<sup>1</sup>)<sup>2-</sup> units, and two oxygen atoms from  $\mu_2$ -acetato ligands (O3 or O3 <sup>#1</sup>). The Ni1 and Ni2 atoms (Ni1 <sup>#1</sup> and Ni2) are connected through  $\mu_2$ -acetato ligands in an usual M-O-C-O-M fashion [66,67]. The coordination sphere around all the Ni<sup>II</sup> atoms are best described as slightly distorted octahedral geometries [68,69]. For the synthesis of Ni<sup>II</sup> coordination compounds must be under dark conditions, the conditions are different from the previously reported Ni<sup>II</sup> coordination compounds [50], the synthesis conditions are different, and the structures of resulting coordination compounds will be changed.

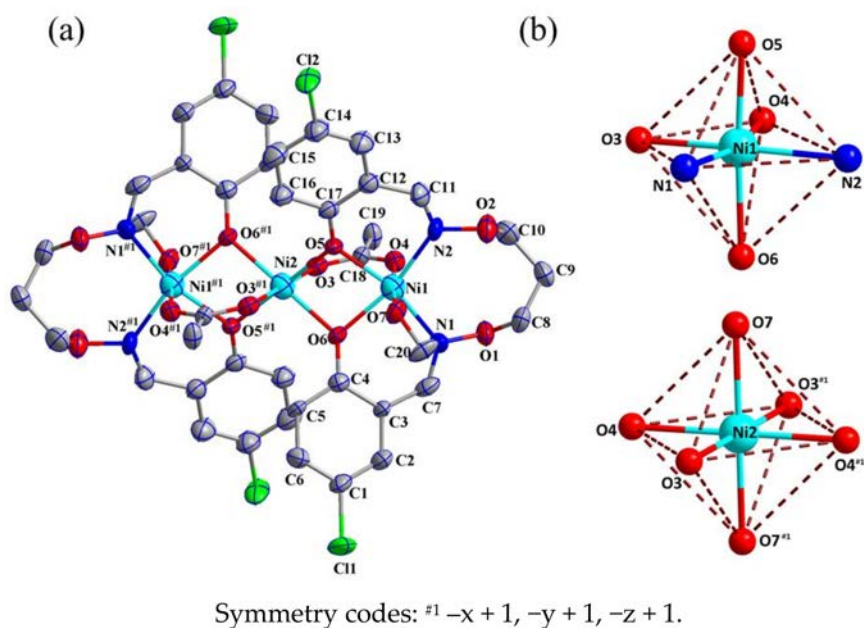


**Figure 3.** (a) Molecular structure and atom numberings of the coordination compound 1 with 30% probability displacement ellipsoids; (b) Coordination polyhedrons for Ni<sup>II</sup> atoms.

The molecular structures and atom numberings of the coordination compounds 2 and 3 are shown in Figures 4 and 5, respectively. Contributions to scattering these highly disordered solvent molecules were removed using the SQUEEZE routine of PLATON. The structure of the coordination compounds 1 was then refined again using the data generated.

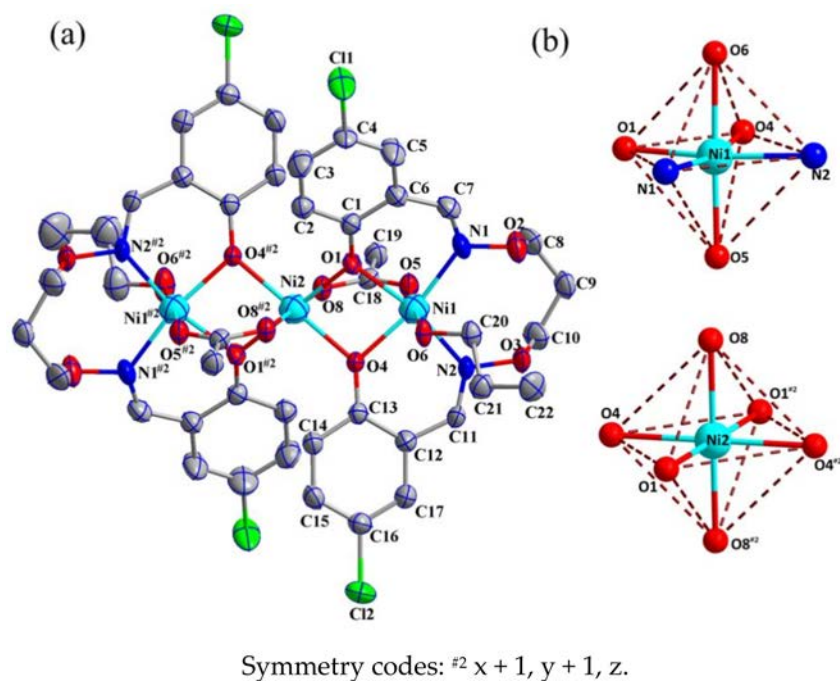


**Figure 4.** (a) Molecular structure and atom numberings of the coordination compound 2 with 30% probability displacement ellipsoids; (b) Coordination polyhedrons for Ni<sup>II</sup> atoms.

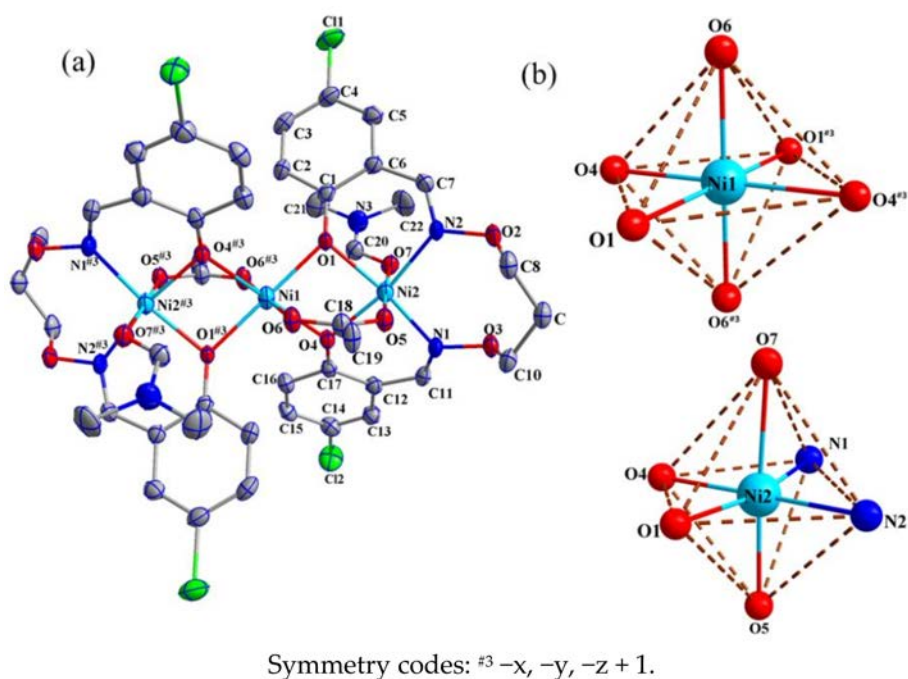


**Figure 5.** (a) Molecular structure and atom numberings of the coordination compound **3** with 30% probability displacement ellipsoids; (b) Coordination polyhedrons for Ni<sup>II</sup> atoms.

In the coordination compound **1**, there are six pairs of the intramolecular C8–H8B···O2, O5–H5···O3, C10–H10B···O6, C3–H3···O7, C10–H10B···O1, and C16–H16···O7 hydrogen bonds are formed (Figure 6) [68,69], and the weak hydrogen bonds existing in the coordination compound **1** has been described in graph sets (Figure 7) [70].

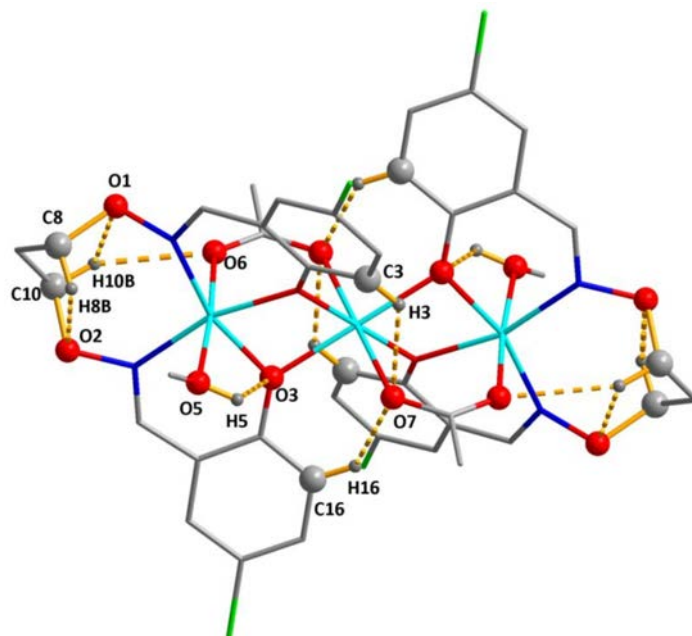


**Figure 6.** View of the intramolecular hydrogen bond interactions of the coordination compound **1**.

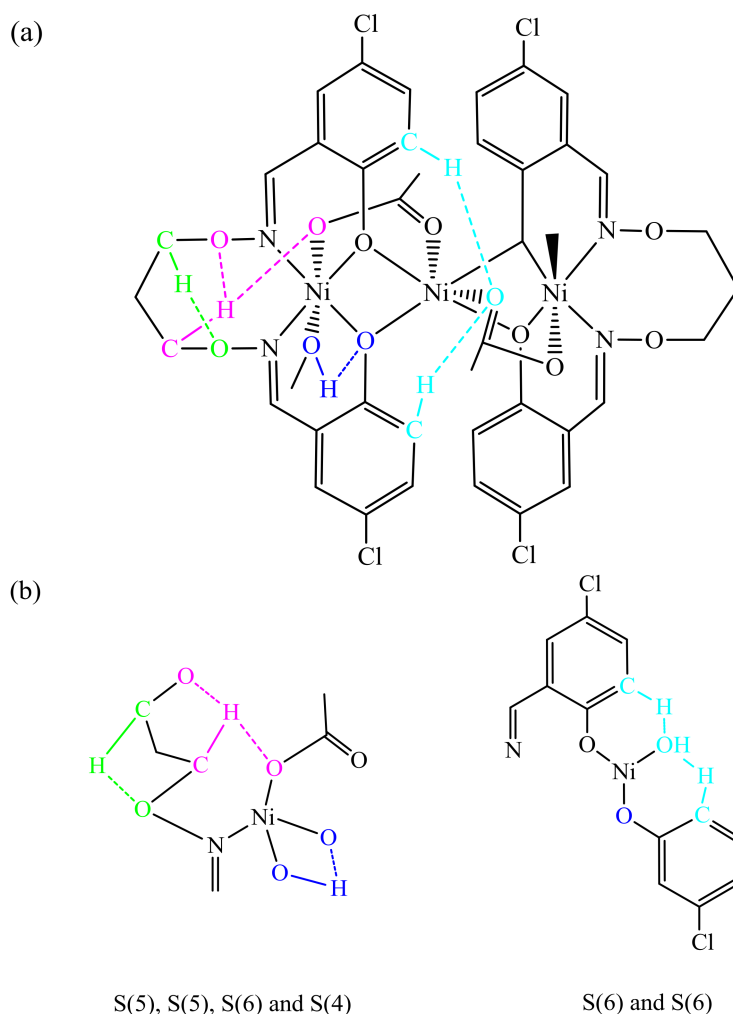


**Figure 7.** (a) Graph set assignments for coordination compound **1**; (b) Partial enlarged drawing of hydrogen bonds.

In the coordination compound **2**, there are three intramolecular hydrogen bonds [68,69] (Figure 8). C8–H8A...O5, O6–H6...O7, and O7–H7A...O8 hydrogen bonds are formed. The donor (C8–H8A) from the  $(L^1)^{2-}$  unit forms hydrogen bond with oxygen atom (O5) of the  $\mu_2$ -acetato ligand as hydrogen bond receptor. The donors (O6–H6 and O7–H7A) from coordinated *n*-propanol molecule and crystalline *n*-propanol molecule form hydrogen bonds with oxygen atoms (O7 and O8) of crystalline *n*-propanol molecule and the  $\mu_2$ -acetato ligand as hydrogen bond receptors. The weak hydrogen bonds existing in the coordination compound **2** have been described in graph sets (Figure 9) [70].

In the coordination compound **3**, there are six pairs of the intramolecular hydrogen bonds (Figure 10) [68,69], and the weak hydrogen bonds existing in the coordination compound **3** have been described in graph sets (Figure 11) [70], C8–H8A...O5, C10–H10B...O5, C20–H20...O6, C22–H22C...O7, C24–H24B...O8 and C24–H24B...O8 hydrogen bonds are formed. The donors (C8–H8A and C10–H10B) come from the  $(L^1)^{2-}$  units form hydrogen bonds with oxygen atom (O5) of the  $\mu_2$ -acetato ligand as hydrogen bond receptor. The donor (C20–H20 and C22–H22C) from the coordinated *N,N*-dimethylformamide molecule form hydrogen bond with oxygen atoms (O6 and O7) of the  $\mu_2$ -acetato ligand and coordinated *N,N*-dimethylformamide molecule as hydrogen bond receptor, and the donor (C24–H24B) from the non-coordinated *N,N*-dimethylformamide molecule form hydrogen bond with oxygen atom (O8) of non-coordinated *N,N*-dimethylformamide molecule as hydrogen bond receptor. As illustrated in Figure 12, the coordination compound **3**

is linked by three pairs of inter-molecular hydrogen bond interactions form a 1D hydrogen bonded chain. In addition, a pair of  $\pi \cdots \pi$  interactions (Cg1  $\cdots$  Cg2 (Cg1=C1-C2-C3-C4-C5-C6 and Cg2=C12-C13-C14-C15-C16-C17)) were formed (Figure 13) [71].

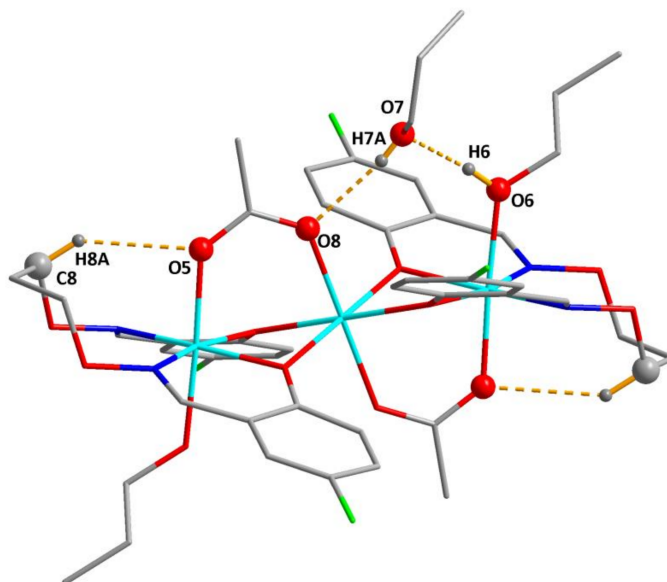


**Figure 8.** View of the intramolecular hydrogen bond interactions of the coordination compound 2.

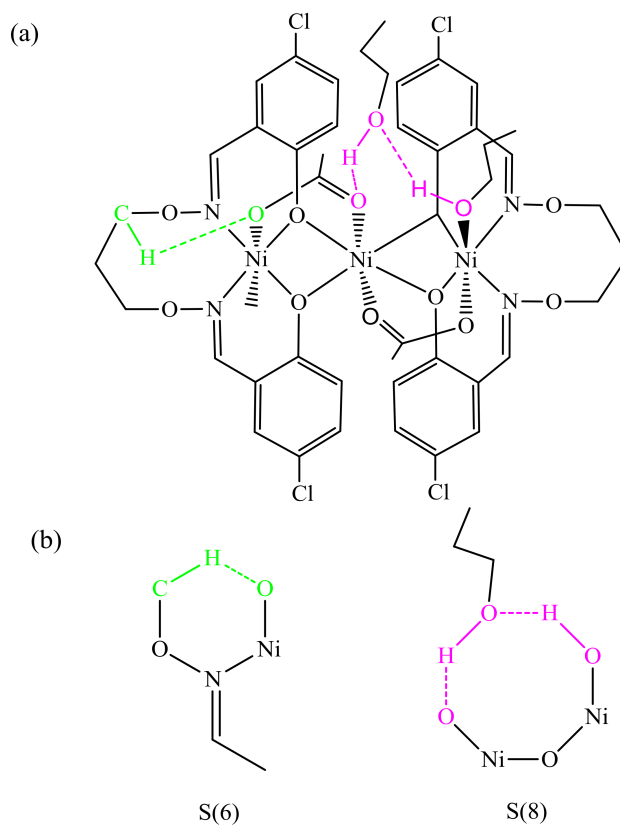


**Figure 9.** (a) Graph set assignments for coordination compound 2; (b) Partial enlarged drawing of hydrogen bonds.

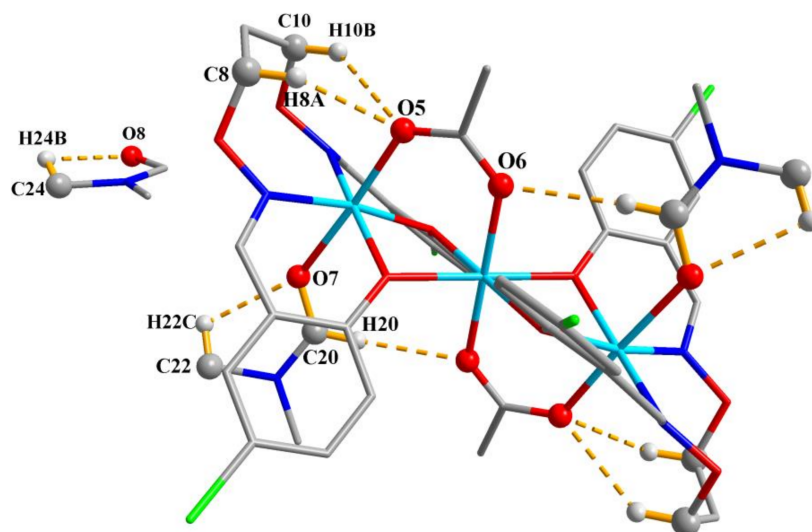


**Figure 10.** View of the intramolecular hydrogen bond interactions of the coordination compound **3**.

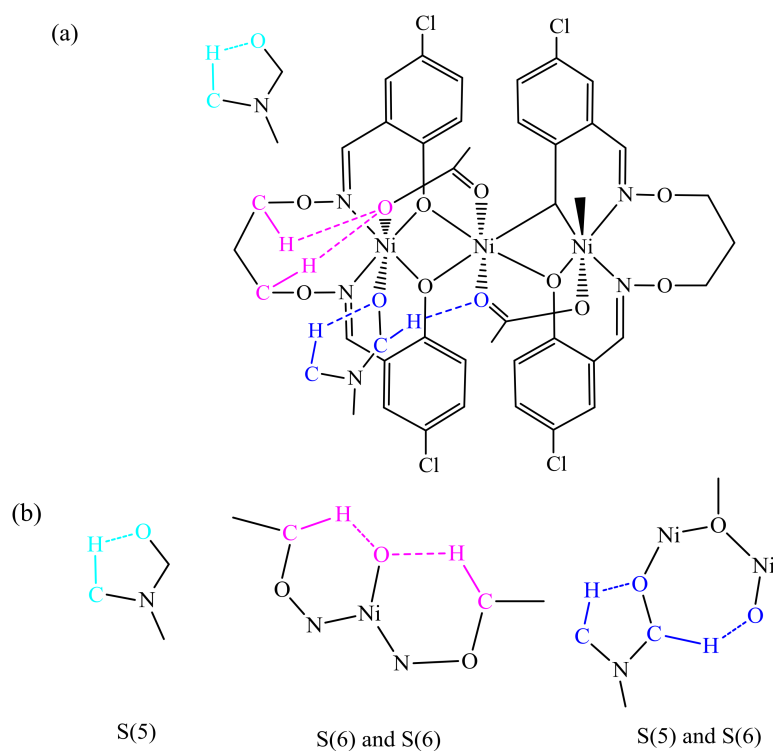


**Figure 11.** (a) Graph set assignments for coordination compound **3**; (b) Partial enlarged drawing of hydrogen bonds.

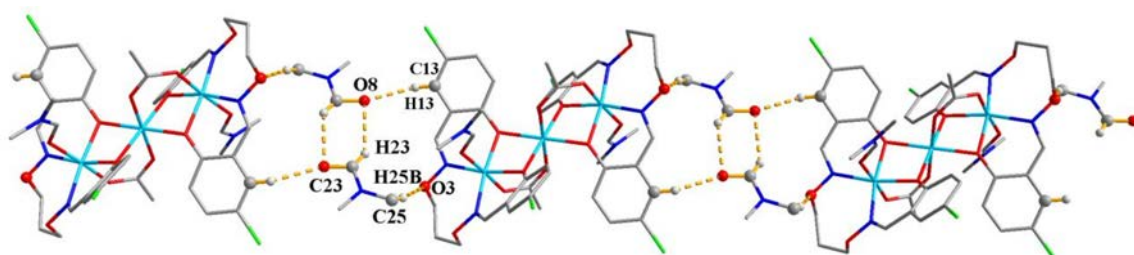


**Figure 12.** View of an infinite 1D hydrogen bonded chain of the coordination compound **3**.

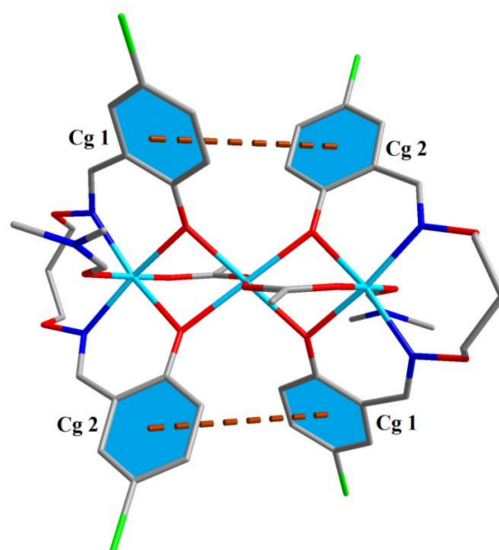
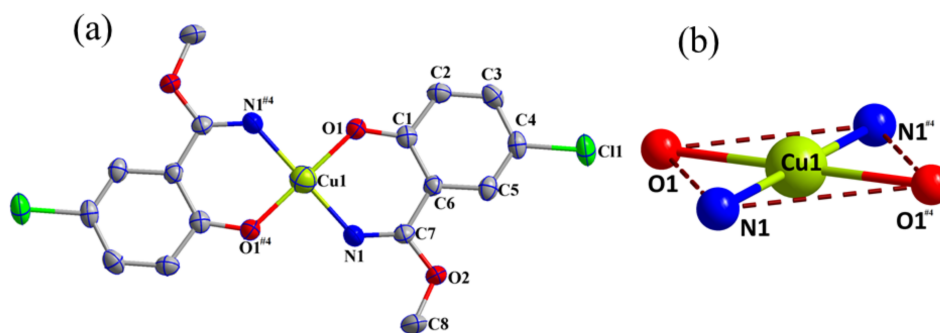


**Figure 13.**  $\pi \cdots \pi$  interactions of coordination compound 3.

### 3.3.2. Crystal Structure of the Coordination Compound 4

Molecular structure of the coordination compound 4 is shown in Figure 14, The structure revealed that the coordination compound 4 crystallizes in the monoclinic system, space group  $C 2/c$ .



Symmetry codes:  $\#4 -x, -y, -z + 1$ .

**Figure 14.** (a) Molecular structure and atom numberings of the coordination compound 4 with 30% probability displacement ellipsoids; (b) Coordination polyhedrons for  $\text{Cu}^{\text{II}}$  atom.

Clearly, the expected mono- or tri-nuclear  $\text{Cu}^{\text{II}}$  coordination compound has not been gained. Catalysis of  $\text{Cu}^{\text{II}}$  ions results in undesigned cleavages of two C–C and two N–O bonds in  $\text{H}_2\text{L}^1$ , and a new coordination compound  $[\text{Cu}(\text{L}^2)_2]$  has been obtained. In C=N bond, the electronegativity of N atom is higher than C atom, so the electron cloud density of C atom is lower. In addition, due to the high electronegativity of Cl atom, the electron cloud density of C atom in C=N bond will be further reduced in this conjugated system, and it is positively charged. If the electronegativity of O atom in the O–C bond is high, it will attack the C atom in C=N bond and form the new ligand  $\text{H}_2\text{L}^2$ . Finally, a new mononuclear  $\text{Cu}^{\text{II}}$  coordination compound has been gained. This phenomenon is not similar to the cleavage of  $\text{Cu}^{\text{II}}$  coordination compounds reported previously [72–74]. In the coordination compound 4, Cu1 atom is four-coordinated and possesses a geometry of slightly distorted planar quadrilateral with two nitrogen atoms of imino and the two phenolic oxygen atoms of the  $(\text{L}^2)^-$  units [72–75]. These angles of N1–Cu1–N1 $^{\#4}$  and O1–Cu1–O1 $^{\#4}$  are all  $180.0^\circ$ . There are two pairs of the intramolecular N1–H1 $\cdots$ O1 and C5–H5 $\cdots$ O2 hydrogen bonds are formed (Figure 15) [72–75]. The weak hydrogen bonds existing in the coordination compound 4 have been described in graph

sets (Figure 16) [70]. As illustrated in Figure 17, the coordination compound **4** is linked by a pair of inter-molecular hydrogen bond interactions forming a 1D hydrogen bonded chain.

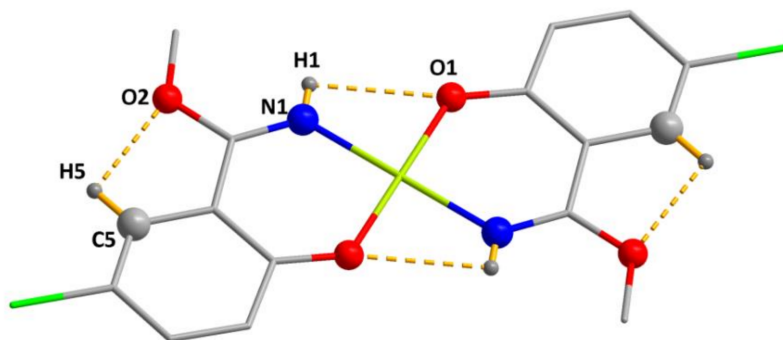


**Figure 15.** View of the intramolecular hydrogen bond interactions of the coordination compound **4**.

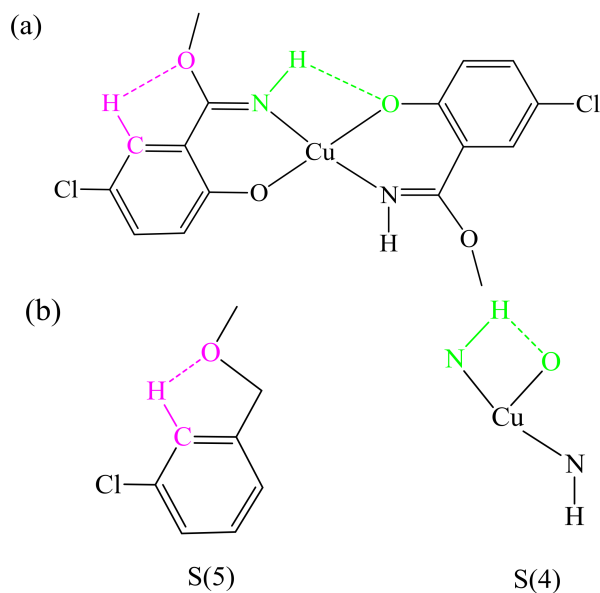


**Figure 16.** (a) Graph set assignments for coordination compound **4**; (b) Partial enlarged drawing of hydrogen bonds.

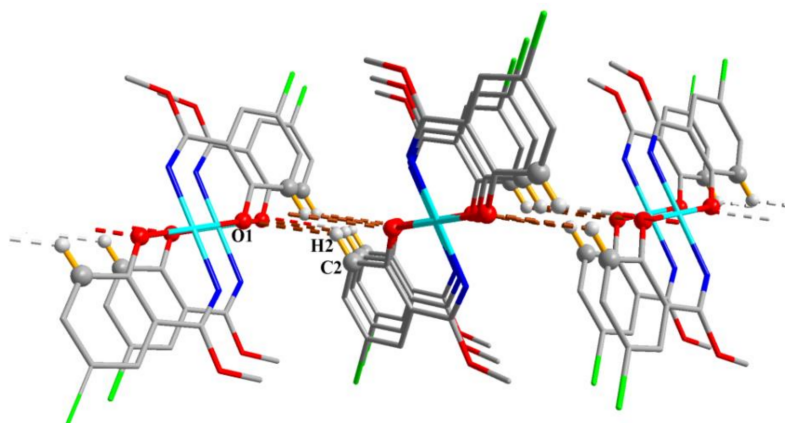


**Figure 17.** View of an infinite 1D hydrogen bonded chain motif of the coordination compound **4** along the *b* axis.

### 3.4. Solvent Effect

Single-crystal X-ray structure analyses revealed that the coordination compounds **1–3** and previously reported coordination compound  $[\text{Ni}_3(\text{L}^1)_2(\text{OAc})_2(\text{CH}_3\text{CH}_2\text{OH})_2] \cdot 2\text{CH}_3\text{CH}_2\text{OH}$  [76] have similar molecular structures, which were affected via the coordinated methanol, n-propanol, *N,N*-dimethylformamide, and ethanol molecules, and the various solvent molecules observed give rise to the formation of the characteristic solvent-induced  $\text{Ni}^{\text{II}}$  coordination compounds. Obviously, the coordination compounds **1**, **2**, **3**, and  $[\text{Ni}_3(\text{L}^1)_2(\text{OAc})_2(\text{CH}_3\text{CH}_2\text{OH})_2] \cdot 2\text{CH}_3\text{CH}_2\text{OH}$  [76] informed different intramolecular hydrogen bond interactions. The effects of solvent molecules are obviously exhibited in selected bond distances (nm) and angles ( $^\circ$ ) for the coordination compounds **1**, **2**, **3**, and  $[\text{Ni}_3(\text{L}^1)_2(\text{OAc})_2(\text{CH}_3\text{CH}_2\text{OH})_2] \cdot 2\text{CH}_3\text{CH}_2\text{OH}$  [76] (Table 2). Because these solvent molecules are different, the distances of Ni1-O5 (**1**), Ni1-O6 (**2**), Ni2-O7 (**3**) and Ni1-O7 ( $[\text{Ni}_3(\text{L}^1)_2(\text{OAc})_2(\text{CH}_3\text{CH}_2\text{OH})_2] \cdot 2\text{CH}_3\text{CH}_2\text{OH}$ ) [76] are 2.099(5), 2.112(3), 2.167(3), and 2.167(4) Å, respectively. The results show that the distances between the metallic ions and the oxygen atoms from the solvent molecules are related to these solvent molecules. Moreover, the dihedral angles of two benzene rings (C1-C6 and C12-C17) in same  $(\text{L}^1)^{2-}$  unit are  $42.80^\circ$  (**1**),  $37.25^\circ$  (**2**), and  $70.35^\circ$  (**3**), respectively (Figures S1–S3). (In the four coordination compounds, coordination compound **1** squeezes out the solvent molecules.) This phenomenon is caused by the difference of solvent molecules. Thus, solvent effects could explain their slight differences in crystal structures.

### 3.5. Fluorescence Behaviors

The fluorescence behaviors of  $\text{H}_2\text{L}^1$  and the coordination compounds **1**, **2**, **3**, and **4** were studied in  $\text{CH}_3\text{OH}$  ( $2.5 \times 10^{-5}$  M) (Figure 18).

The ligand  $\text{H}_2\text{L}^1$  demonstrates a strong emission peak at ca. 507 nm upon excitation at 324 nm, which could be attributed to the intraligand  $\pi$ - $\pi^*$  transition [72,73]. The coordination compounds **1**, **2**, **3**, and **4** demonstrate weak photoluminescence with maximum emissions at ca. 519, 523, 522 and 521 nm upon excitation at 378 nm (based on global maxima determined from three-dimensional fluorescence spectra), respectively, and the peaks are bathochromically shifted, which should be attributed to ligand-to-metal charge transfer (LMCT) [74,75]. Compared with  $\text{H}_2\text{L}^1$ , the emission intensities of the coordination compounds **1**, **2**, **3**, and **4** are reduced, which indicate that the  $\text{Ni}^{\text{II}}$  and  $\text{Cu}^{\text{II}}$  ions have the behaviors of fluorescent quenching, and the quenching of  $\text{Cu}^{\text{II}}$  ion is more obvious than that of  $\text{Ni}^{\text{II}}$  ion.

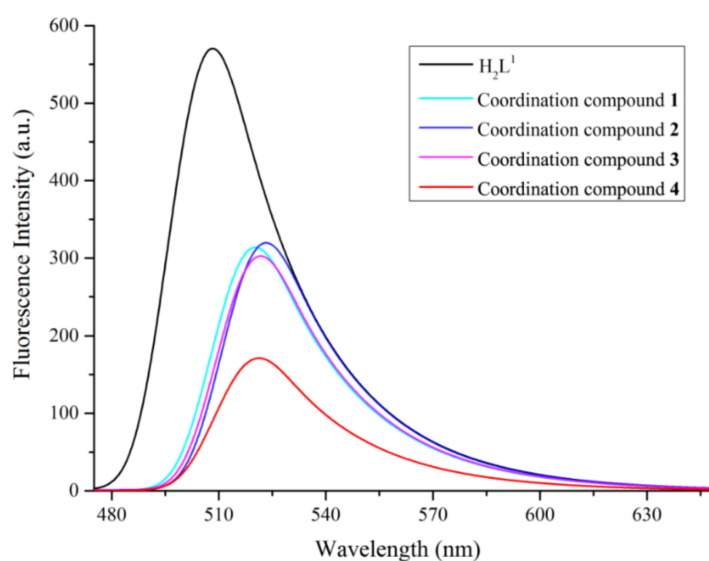


**Figure 18.** Emission spectra of  $\text{H}_2\text{L}^1$  ( $\lambda_{\text{ex}} = 324$  nm) and the coordination compounds **1–4** ( $\lambda_{\text{ex}} = 378$  nm) in  $\text{CH}_3\text{OH}$  ( $2.5 \times 10^{-5}$  M).

### 3.6. Magnetic Behavior

The magnetic behaviors of the coordination compound **1** were measured and discussed individually represented the coordination compounds **2** and **3**, owing to these coordination compounds have analogous structures, there are little difference in magnetic behavior. The temperature dependence of magnetic susceptibilities of the coordination compound **1** is depicted in Figure 19.

The  $\chi_M T$  value at 300 K for the coordination compound **1** is  $3.28 \text{ cm}^3 \text{ K mol}^{-1}$ , which is higher than the value of  $3 \text{ cm}^3 \text{ K mol}^{-1}$  expected for three  $\text{Ni}^{\text{II}}$  ( $S = 1$ ) magnetically isolated ions [77–79]. Upon lowering the temperature, the  $\chi_M T$  value of the coordination compound **1** gradually decreases to reach a minimum value of  $0.60 \text{ cm}^3 \text{ K mol}^{-1}$  at 2 K, which shows that a weak antiferromagnetic interaction exists in such a coordination compound [80]. Moreover, the magnetic susceptibilities ( $1/\chi_M$ ) obey the Curie–Weiss law ( $\chi_M = C/(T - \theta)$ ) in the 2–300 K temperature range, giving a negative Weiss constant  $\theta = -14.220 \text{ K}$  and  $C = 3.466 \text{ cm}^3 \text{ K mol}^{-1}$  (Figure 19, inset) and confirming the antiferromagnetic interaction presented again by the coordination compound **1** [80].

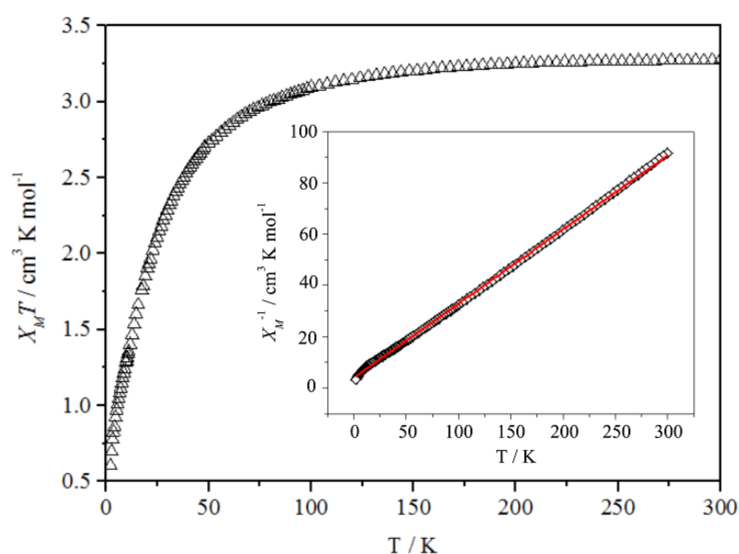


**Figure 19.** Plots of  $\chi_M T$  vs.  $T$  for the coordination compound **1** between 2 to 300 K. Inset: Temperature dependence of  $\chi_M^{-1}$ . The red solid lines show the best fitting results.

## 4. Conclusions

Different solvent molecules were introduced, three new homotrimeric  $\text{Ni}^{\text{II}}$  coordination compounds **1**, **2**, and **3** with a salamo-like bisoxime ligand  $\text{H}_2\text{L}^1$  were designed and synthesized. Catalysis of  $\text{Cu}^{\text{II}}$  ions results in undesigned cleavage of two C–C and two N–O bonds in  $\text{H}_2\text{L}^1$ . A new mono-nuclear  $\text{Cu}^{\text{II}}$  coordination compound  $[\text{Cu}(\text{L}^2)_2]$  has been obtained. Single-crystal X-ray crystal structure analyses revealed that the coordination compounds **1–3** have analogous molecular structures and were affected by the coordinated methanol, n-propanol, and *N,N*-dimethylformamide molecules, respectively, and the virous solvent molecules observed give rise to the formation of the characteristic solvent-induced  $\text{Ni}^{\text{II}}$  coordination compounds. All the  $\text{Ni}^{\text{II}}$  atoms are six-coordinated with geometries of slightly distorted octahedron. Obviously, the expected mono- or tri-nuclear  $\text{Cu}^{\text{II}}$  coordination compound has not been gained, but a new  $\text{Cu}^{\text{II}}$  coordination compound  $[\text{Cu}(\text{L}^2)_2]$  has been obtained. In coordination compound **4**, the Cu1 atom is four-coordinated with a geometry of slightly distorted planar quadrilateral. The fluorescent behavior of  $\text{H}_2\text{L}^1$  and the coordination compounds **1–4** were studied. Compared with  $\text{H}_2\text{L}^1$ , the emission intensities of the coordination compounds **1–4** decreases clearly, which exhibits that the  $\text{Ni}^{\text{II}}$  and  $\text{Cu}^{\text{II}}$  ions bear the qualities of fluorescence quenching, and the quenching of  $\text{Cu}^{\text{II}}$  ion is more obvious than that of  $\text{Ni}^{\text{II}}$  ion. In addition, the magnetic behavior showed that there is a relatively weak antiferromagnetic interaction in coordination compound **1**.

**Supplementary Materials:** The following are available online at <http://www.mdpi.com/2073-4352/8/4/173/s1>, Figure S1: View of the dihedral angles between two benzene rings (C1-C6 and C12-C17) of the coordination compound **1**, Figure S2: View of the dihedral angles between two benzene rings (C1-C6 and C12-C17) of the coordination compound **2**, Figure S3: View of the dihedral angles between two benzene rings (C1-C6 and C12-C17) of the coordination compound **3**.

**Acknowledgments:** This work was supported by the National Natural Science Foundation of China (21761018) and the Program for Excellent Team of Scientific Research in Lanzhou Jiaotong University (201706), both of which are gratefully acknowledged.

**Author Contributions:** Wen-Kui Dong and Quan-Peng Kang conceived and designed the experiments; Xiao-Yan Li and Ling-Zhi Liu performed the experiments; Jian-Chun Ma analyzed the data; Wen-Kui Dong and Lin-Wei Zhang contributed reagents/materials/analysis tools; Lin-Wei Zhang and Xiao-Yan Li wrote the paper.

**Conflicts of Interest:** The authors declare no competing financial interests.

## References

1. Sun, Y.X.; Xu, L.; Zhao, T.H.; Liu, S.H.; Liu, G.H.; Dong, X.T. Synthesis and crystal structure of a 3D supramolecular copper(II) complex with 1-(3-[(E)-3-bromo-5-chloro-2-hydroxybenzylidene]amino)phenyl) ethanone oxime. *Synth. React. Inorg. Met.-Org. Nano-Met. Chem.* **2013**, *43*, 509–513. [[CrossRef](#)]
2. Sun, Y.X.; Zhang, Y.J.; Meng, W.S.; Li, X.R.; Lu, R.E. Synthesis and crystal structure of new nickel(II) complex with Salen-type bisoxime ligand. *Asian J. Chem.* **2014**, *26*, 416–418.
3. Song, X.Q.; Liu, P.P.; Xiao, Z.R.; Li, X.; Liu, Y.A. Four polynuclear complexes based on a versatile salicylamide salen-like ligand: Synthesis, structural variations and magnetic properties. *Inorg. Chim. Acta* **2015**, *438*, 232–244. [[CrossRef](#)]
4. Sun, Y.X.; Gao, X.H. Synthesis, characterization, and crystal structure of a new Cu<sup>II</sup> complex with salen-type ligand. *Synth. React. Inorg. Met.-Org. Nano-Met. Chem.* **2011**, *41*, 973–978. [[CrossRef](#)]
5. Li, L.H.; Dong, W.K.; Zhang, Y.; Akogun, S.F.; Xu, L. Syntheses, structures and catecholase activities of homo- and hetero-trinuclear cobalt(II) complexes constructed from an acyclic naphthalenediol-based bis(salamo)-type ligand. *Appl. Organomet. Chem.* **2017**, *31*, e3818. [[CrossRef](#)]
6. Li, X.Y.; Chen, L.; Gao, L.; Zhang, Y.; Akogun, S.F.; Dong, W.K. Syntheses, crystal structures and catalytic activities of two solvent-induced homotrimeric Co(II) complexes with a naphthalenediol-based bis(Salamo)-type tetraoxime ligand. *RSC Adv.* **2017**, *7*, 35905–35916. [[CrossRef](#)]
7. Ene, C.D.; Nastase, S.; Maxim, C.; Madalan, A.M.; Tuna, F.; Andruh, M. The azidopentacyanoferrate(III) ion as a tecton in constructing heterometallic complexes: Synthesis, crystal structure and magnetic properties of [Mn(valphen)(H<sub>2</sub>O)<sub>2</sub>]<sub>2</sub>[(H<sub>2</sub>O)(valphen)Mn(μ-CN)Fe(CN)<sub>4</sub>(N<sub>3</sub>)]·8H<sub>2</sub>O. *Inorg. Chim. Acta* **2010**, *363*, 4247–4252. [[CrossRef](#)]
8. Dong, W.K.; Ma, J.C.; Dong, Y.J.; Zhu, L.C.; Zhang, Y. Di- and tetranuclear heterometallic 3d–4f cobalt(II)–lanthanide(III) complexes derived from a hexadentate bisoxime: Syntheses, structures and magnetic properties. *Polyhedron* **2016**, *115*, 228–235. [[CrossRef](#)]
9. Liu, P.P.; Sheng, L.; Song, X.Q.; Xu, W.Y.; Liu, Y.A. Synthesis, structure and magnetic properties of a new one dimensional manganese coordination polymer constructed by a new asymmetrical ligand. *Inorg. Chim. Acta* **2015**, *434*, 252–257. [[CrossRef](#)]
10. Song, X.Q.; Liu, P.P.; Liu, Y.A.; Zhou, J.J.; Wang, X.L. Two dodecanuclear heterometallic [Zn<sub>6</sub>Ln<sub>6</sub>] clusters constructed by a multidentate salicylamide salen-like ligand: Synthesis, structure, luminescence and magnetic properties. *Dalton Trans.* **2016**, *45*, 8154–8163. [[CrossRef](#)] [[PubMed](#)]
11. Wu, H.L.; Pan, G.L.; Wang, H.; Wang, X.L.; Bai, Y.C.; Zhang, Y.H. Study on synthesis, crystal structure, antioxidant and DNA-binding of mono-, di- and poly-nuclear lanthanides complexes with bis(*N*-salicylidene)-3-oxapentane-1,5-diamine. *J. Photochem. Photobiol. B* **2014**, *135*, 33–43. [[CrossRef](#)] [[PubMed](#)]
12. Wu, H.L.; Pan, G.L.; Bai, Y.C.; Wang, H.; Kong, J.; Shi, F.; Zhang, Y.H.; Wang, X.L. Preparation, structure, DNA-binding properties, and antioxidant activities of a homodinuclear erbium(III) complex with a pentadentate Schiff base ligand. *J. Chem. Res.* **2014**, *38*, 211–217. [[CrossRef](#)]
13. Wu, H.L.; Bai, Y.; Yuan, J.K.; Wang, H.; Pan, G.L.; Fan, X.Y.; Kong, J. A zinc(II) complex with tris(2-(*N*-methyl)benzimidazolylmethyl)amine and salicylate: Synthesis, crystal structure, and DNA-binding. *J. Coord. Chem.* **2012**, *65*, 2839–2851. [[CrossRef](#)]

14. Wu, H.L.; Bai, Y.C.; Zhang, Y.H.; Pan, G.L.; Kong, J.; Shi, F.; Wang, X.L. Two lanthanide(III) complexes based on the schiff base *N,N*-Bis(salicylidene)-1,5-diamino-3-oxapentane: Synthesis, characterization, DNA-binding properties, and antioxidation. *Z. Anorg. Allg. Chem.* **2014**, *640*, 2062–2071. [[CrossRef](#)]
15. Chen, C.Y.; Zhang, J.W.; Zhang, Y.H.; Yang, Z.H.; Wu, H.L. Gadolinium(III) and dysprosium(III) complexes with a Schiff base bis(*N*-salicylidene)-3-oxapentane-1,5-diamine: Synthesis, characterization, antioxidation, and DNA-binding studies. *J. Coord. Chem.* **2015**, *68*, 1054–1071. [[CrossRef](#)]
16. Wu, H.L.; Wang, C.P.; Wang, F.; Peng, H.P.; Zhang, H.; Bai, Y.C. A new manganese(III) complex from bis(5-methylsalicylaldehyde)-3-oxapentane-1,5-diamine: Synthesis, characterization, antioxidant activity and luminescence. *J. Chin. Chem. Soc.* **2015**, *62*, 1028–1034. [[CrossRef](#)]
17. Wu, H.L.; Pan, G.L.; Bai, Y.C.; Wang, H.; Kong, J. Synthesis, structure, antioxidation, and DNA-binding studies of a binuclear ytterbium(III) complex with bis(*N*-salicylidene)-3-oxapentane-1,5-diamine. *Res. Chem. Intermed.* **2015**, *41*, 3375–3388. [[CrossRef](#)]
18. Dong, W.K.; Ma, J.C.; Zhu, L.C.; Zhang, Y. Nine self-assembled nickel(II)–lanthanide(III) heterometallic complexes constructed from a Salamo-type bisoxime and bearing N- or O-donor auxiliary ligand: Syntheses, structures and magnetic properties. *New J. Chem.* **2016**, *40*, 6998–7010. [[CrossRef](#)]
19. Sun, Y.X.; Zhang, S.T.; Ren, Z.L.; Dong, X.Y.; Wang, L. Synthesis, characterization, and crystal structure of a new supramolecular Cd<sup>II</sup> complex with halogen-substituted salen-type bisoxime. *Synth. React. Inorg. Met.-Org. Nano-Met. Chem.* **2013**, *43*, 995–1000. [[CrossRef](#)]
20. Zhao, L.; Dang, X.T.; Chen, Q.; Zhao, J.X.; Wang, L. Synthesis, crystal structure and spectral properties of a 2D supramolecular copper(II) complex with 1-(4-((*E*)-3-ethoxyl-2-hydroxybenzylidene)amino)phenyl)ethanone oxime. *Synth. React. Inorg. Met.-Org. Nano-Met. Chem.* **2013**, *43*, 1241–1246. [[CrossRef](#)]
21. Sun, Y.X.; Wang, L.; Dong, X.Y.; Ren, Z.L.; Meng, W.S. Synthesis, characterization, and crystal structure of a supramolecular Co<sup>II</sup> complex containing Salen-type bisoxime. *Synth. React. Inorg. Met.-Org. Nano-Met. Chem.* **2013**, *43*, 599–603. [[CrossRef](#)]
22. Dong, W.K.; Li, X.L.; Wang, L.; Zhang, Y.; Ding, Y.J. A new application of Salamo-type bisoximes: As a relay-sensor for Zn<sup>2+</sup>/Cu<sup>2+</sup> and its novel complexes for successive sensing of H<sup>+</sup>/OH<sup>−</sup>. *Sens. Actuators B* **2016**, *229*, 370–378. [[CrossRef](#)]
23. Dong, W.K.; Akogun, S.F.; Zhang, Y.; Sun, Y.X.; Dong, X.Y. A reversible “turn-on” fluorescent sensor for selective detection of Zn<sup>2+</sup>. *Sens. Actuators B* **2017**, *238*, 723–734. [[CrossRef](#)]
24. Wang, B.J.; Dong, W.K.; Zhang, Y.; Akogun, S.F. A novel relay-sensor for highly sensitive and selective detection of Zn<sup>2+</sup>/Pic<sup>−</sup> and fluorescence on/off switch response of H<sup>+</sup>/OH<sup>−</sup>. *Sens. Actuators B* **2017**, *247*, 254–264. [[CrossRef](#)]
25. Wang, F.; Gao, L.; Zhao, Q.; Zhang, Y.; Dong, W.K.; Ding, Y.J. A highly selective fluorescent chemosensor for CN<sup>−</sup> based on a novel bis(salamo)-type tetraoxime ligand. *Spectrochim. Acta Part A* **2018**, *190*, 111–115. [[CrossRef](#)] [[PubMed](#)]
26. Chai, L.Q.; Liu, G.; Zhang, Y.L.; Huang, J.J.; Tong, J.F. Synthesis, crystal structure, fluorescence, electrochemical property, and SOD-like activity of an unexpected nickel(II) complex with a quinazoline-type ligand. *J. Coord. Chem.* **2013**, *66*, 3926–3938. [[CrossRef](#)]
27. Dong, W.K.; Lan, P.F.; Zhou, W.M.; Zhang, Y. Salamo-type trinuclear and tetranuclear cobalt(II) complexes based on a new asymmetry Salamoto-type ligand: Syntheses, crystal structures, and fluorescence properties. *J. Coord. Chem.* **2016**, *69*, 1272–1283. [[CrossRef](#)]
28. Dong, W.K.; Zhang, J.; Zhang, Y.; Li, N. Novel multinuclear transition metal(II) complexes based on an asymmetric salamo-type ligand: Syntheses, structure characterizations and fluorescent properties. *Inorg. Chim. Acta* **2016**, *444*, 95–102. [[CrossRef](#)]
29. Song, X.Q.; Zheng, Q.F.; Wang, L.; Liu, W.S. Synthesis and luminescence properties of lanthanide complexes with a new tripodal ligand featuring *N*-thenylsalicylamide arms. *Luminescence* **2012**, *27*, 459–465. [[CrossRef](#)] [[PubMed](#)]
30. Dong, W.K.; Ma, J.C.; Zhu, L.C.; Zhang, Y. Self-assembled zinc(II)–lanthanide(III) heteromultinuclear complexes constructed from 3-MeOsalamo ligand: Syntheses, structures and luminescent properties. *Cryst. Growth Des.* **2016**, *16*, 6903–6914. [[CrossRef](#)]
31. Chai, L.Q.; Tang, L.J.; Chen, L.C.; Huang, J.J. Structural, spectral, electrochemical and DFT studies of two mononuclear manganese(II) and zinc(II) complexes. *Polyhedron* **2017**, *122*, 228–240. [[CrossRef](#)]

32. Chai, L.Q.; Zhang, K.Y.; Tang, L.J.; Zhang, J.Y.; Zhang, H.S. Two mono- and dinuclear Ni(II) complexes constructed from quinazoline-type ligands: Synthesis, X-ray structures, spectroscopic, electrochemical, thermal, and antimicrobial studies. *Polyhedron* **2017**, *130*, 100–107. [[CrossRef](#)]
33. Hao, J.; Li, L.L.; Zhang, J.T.; Akogun, S.F.; Wang, L.; Dong, W.K. Four homo- and hetero-bimetallic 3d/3d-2s complexes constructed from a naphthalenediol-based acyclic bis(salamo)-type tetraoxime ligand. *Polyhedron* **2017**, *134*, 1–10. [[CrossRef](#)]
34. Song, X.Q.; Wang, L.; Zheng, Q.F.; Liu, W.S. Synthesis, crystal structure and luminescence properties of lanthanide complexes with a new semirigid bridging furfurylsalicylamide ligand. *Inorg. Chim. Acta* **2012**, *391*, 171–178. [[CrossRef](#)]
35. Liu, Y.A.; Wang, C.Y.; Zhang, M.; Song, X.Q. Structures and magnetic properties of cyclic heterometallic tetranuclear clusters. *Polyhedron* **2017**, *127*, 278–286. [[CrossRef](#)]
36. Song, X.Q.; Peng, Y.J.; Chen, G.Q.; Wang, X.R.; Liu, P.P.; Xu, W.Y. Substituted group-directed assembly of Zn(II) coordination complexes based on two new structural related pyrazolone based Salen ligands: Syntheses, structures and fluorescence properties. *Inorg. Chim. Acta* **2015**, *427*, 13–21. [[CrossRef](#)]
37. Dong, X.Y.; Li, X.Y.; Liu, L.Z.; Zhang, H.; Ding, Y.J.; Dong, W.K. Tri- and hexanuclear heterometallic Ni(II)–M(II) (M = Ca, Sr and Ba) bis(salamo)-type complexes: Synthesis, structure and fluorescence properties. *RSC Adv.* **2017**, *7*, 48394–48403. [[CrossRef](#)]
38. Li, G.; Hao, J.; Liu, L.Z.; Zhou, W.M.; Dong, W.K. Syntheses, crystal structures and thermal behaviors of two supramolecular salamo-type cobalt(II) and zinc(II) complexes. *Crystals* **2017**, *7*, 217. [[CrossRef](#)]
39. Song, X.Q.; Lei, Y.K.; Wang, X.R.; Zhao, M.M.; Peng, Y.Q.; Cheng, G.Q. Lanthanide coordination polymers: Synthesis, diverse structure and luminescence properties. *J. Solid State Chem.* **2014**, *218*, 202–212. [[CrossRef](#)]
40. Dong, Y.J.; Dong, X.Y.; Dong, W.K.; Zhang, Y.; Zhang, L.S. Three asymmetric Salamo-type copper(II) and cobalt(II) complexes: Syntheses, structures, fluorescent properties. *Polyhedron* **2017**, *123*, 305–315. [[CrossRef](#)]
41. Dong, X.Y.; Akogun, S.F.; Zhou, W.M.; Dong, W.K. Tetranuclear Zn(II) complex based on an asymmetrical Salamo-type chelating ligand: Synthesis, structural characterization, and fluorescence property. *J. Chin. Chem. Soc.* **2017**, *64*, 412–419. [[CrossRef](#)]
42. Zhao, L.; Wang, L.; Sun, Y.X.; Dong, W.K.; Tang, X.L.; Gao, X.H. A supramolecular copper(II) complex bearing salen-type bisoxime ligand: Synthesis, structural characterization, and thermal property. *Synth. React. Inorg. Met.-Org. Nano-Met. Chem.* **2012**, *42*, 1303–1308. [[CrossRef](#)]
43. Zheng, S.S.; Dong, W.K.; Zhang, Y.; Chen, L.; Ding, Y.J. Four Salamo-type 3d–4f hetero-bimetallic [Zn<sup>II</sup>Ln<sup>III</sup>] complexes: Syntheses, crystal structures, and luminescent and magnetic properties. *New J. Chem.* **2017**, *41*, 4966–4973. [[CrossRef](#)]
44. Akine, S.; Taniguchi, T.; Nabeshima, T. Acyclic bis(N<sub>2</sub>O<sub>2</sub> chelate) ligand for trinuclear d-block homo- and heterometal complexes. *Inorg. Chem.* **2008**, *47*, 3255–3264. [[CrossRef](#)] [[PubMed](#)]
45. Ren, Z.L.; Wang, F.; Liu, L.Z.; Jin, B.X.; Dong, W.K. Unprecedented hexanuclear cobalt(II) nonsymmetrical salamo-based coordination compound: Synthesis, crystal structure, and photophysical properties. *Crystals* **2018**, *8*, 144.
46. Dong, W.K.; Shi, J.Y.; Zhong, J.K.; Sun, Y.X.; Duan, J.G. Synthesis and structural characterization of a novel tricobalt cluster with 4,4'-dichloro-2,2'-(1,3-propylene)dioxybis(nitrilomethylidyne)diphenol. *Struct. Chem.* **2008**, *19*, 95–99. [[CrossRef](#)]
47. Dong, W.K.; Yao, J.; Sun, Y.X. Synthesis, characterization, and crystal structure of a tri-nuclear cobalt(II) cluster. *Synth. React. Inorg. Met.-Org. Nano-Met. Chem.* **2011**, *41*, 177–181.
48. Wu, H.L.; Bai, Y.C.; Zhang, Y.H.; Li, Z.; Wu, M.C.; Chen, C.Y.; Zhang, J.W. Synthesis, crystal structure, antioxidation and DNA-binding properties of a dinuclear copper(II) complex with bis(N-salicylidene)-3-oxapentane-1, 5-diamine. *J. Coord. Chem.* **2014**, *67*, 3054–3066. [[CrossRef](#)]
49. Dong, W.K.; Duan, J.G.; Guan, Y.H.; Shi, J.Y.; Zhao, C.Y. Synthesis, crystal structure and spectroscopic behaviors of Co(II) and Cu(II) complexes with Salen-type bisoxime ligands. *Inorg. Chim. Acta* **2009**, *362*, 1129–1134. [[CrossRef](#)]
50. Li, X.Y.; Kang, Q.P.; Liu, L.Z.; Ma, J.C.; Dong, W.K. Trinuclear Co(II) and mononuclear Ni(II) Salamo-type bisoxime coordination compounds. *Crystals* **2018**, *8*, 43. [[CrossRef](#)]
51. Akine, S.; Taniguchi, T.; Dong, W.K.; Masubuchi, S.; Nabeshima, T. Oxime-based Salen-type tetradentate ligands with high stability against imine metathesis reaction. *J. Org. Chem.* **2005**, *70*, 1704–1711. [[CrossRef](#)] [[PubMed](#)]

52. Sheldrick, G.M. *Program for Crystal Structure Solution*; SHELXS-2008; University of Göttingen: Göttingen, Germany, 2008.
53. Sheldrick, G.M. *Program for Crystal Structure Refinement*; SHELXL-2008; University of Göttingen: Göttingen, Germany, 2008.
54. Gao, L.; Wang, F.; Zhao, Q.; Zhang, Y.; Dong, W.K. Mononuclear Zn(II) and trinuclear Ni(II) complexes derived from a coumarin-containing N<sub>2</sub>O<sub>2</sub> ligand: Syntheses, crystal structures and fluorescence properties. *Polyhedron* **2018**, *139*, 7–16. [[CrossRef](#)]
55. Wang, P.; Zhao, L. An infinite 2D supramolecular cobalt(II) complex based on an asymmetric Salamo-type ligand: Synthesis, crystal structure, and spectral properties. *Synth. React. Inorg. Met.-Org. Nano-Met. Chem.* **2016**, *46*, 1095–1101. [[CrossRef](#)]
56. Wang, L.; Hao, J.; Zhai, L.X.; Zhang, Y.; Dong, W.K. Synthesis, crystal structure, luminescence, electrochemical and antimicrobial properties of bis(salamo)-based Co(II) complex. *Crystals* **2017**, *7*, 277. [[CrossRef](#)]
57. Wang, L.; Ma, J.C.; Dong, W.K.; Zhu, L.C.; Zhang, Y. A novel Self-assembled nickel(II)–cerium(III) heterotetranuclear dimer constructed from N<sub>2</sub>O<sub>2</sub>-type bisoxime and terephthalic acid: Synthesis, structure and photophysical properties. *Z. Anorg. Allg. Chem.* **2016**, *642*, 834–839. [[CrossRef](#)]
58. Dong, X.Y.; Sun, Y.X.; Wang, L.; Li, L. Synthesis and structure of a penta- and hexa-coordinated tri-nuclear cobalt(II) complex. *J. Chem. Res.* **2012**, *36*, 387–390. [[CrossRef](#)]
59. Dong, X.Y.; Gao, L.; Wang, F.; Zhang, Y.; Dong, W.K. Tri- and mono-nuclear zinc(II) complexes based on half- and mono-salamo chelating ligands. *Crystals* **2017**, *7*, 267. [[CrossRef](#)]
60. Wang, L.; Li, X.Y.; Zhao, Q.; Li, L.H.; Dong, W.K. Fluorescence properties of heterotrinuclear Zn(II)–M(II) (M = Ca, Sr and Ba) bis(salamo)-type complexes. *RSC Adv.* **2017**, *7*, 48730–48737. [[CrossRef](#)]
61. Dong, W.K.; Ma, J.C.; Zhu, L.C.; Zhang, Y.; Li, X.L. Four new nickel(II) complexes based on an asymmetric Salamo-type ligand: Synthesis, structure, solvent effect and electrochemical property. *Inorg. Chim. Acta* **2016**, *445*, 140–148. [[CrossRef](#)]
62. Yang, Y.H.; Hao, J.; Dong, Y.J.; Wang, G.; Dong, W.K. Two zinc(II) complexes constructed from a bis(salamo)-type tetraoxime ligand: Syntheses, crystal structures and luminescence properties. *Chin. J. Inorg. Chem.* **2017**, *33*, 1280–1292.
63. Xu, L.; Zhu, L.C.; Ma, J.C.; Zhang, Y.; Zhang, J.; Dong, W.K. Syntheses, structures and spectral properties of mononuclear Cu<sup>II</sup> and dimeric Zn<sup>II</sup> complexes based on an asymmetric Salamo-type N<sub>2</sub>O<sub>2</sub> ligand. *Z. Anorg. Allg. Chem.* **2015**, *641*, 2520–2524. [[CrossRef](#)]
64. Tao, C.H.; Ma, J.C.; Zhu, L.C.; Zhang, Y.; Dong, W.K. Heterobimetallic 3d–4f Zn(II)–Ln(III) (Ln = Sm, Eu, Tb and Dy) complexes with a N<sub>2</sub>O<sub>4</sub> bisoxime chelate ligand and a simple auxiliary ligand Py: Syntheses, structures and luminescence properties. *Polyhedron* **2017**, *128*, 38–45. [[CrossRef](#)]
65. Dong, Y.J.; Ma, J.C.; Zhu, L.C.; Dong, W.K.; Zhang, Y. Four 3d–4f heteromultinuclear zinc(II)–lanthanide(III) complexes constructed from a distinct hexadentate N<sub>2</sub>O<sub>2</sub>-type ligand: Syntheses, structures and photophysical properties. *J. Coord. Chem.* **2017**, *70*, 103–115. [[CrossRef](#)]
66. Dong, W.K.; Zhang, J.T.; Dong, Y.J.; Zhang, Y.; Wang, Z.K. Construction of mononuclear copper(II) and trinuclear cobalt(II) complexes based on asymmetric Salamo-type ligands. *Z. Anorg. Allg. Chem.* **2016**, *642*, 189–196. [[CrossRef](#)]
67. Wang, P.; Zhao, L. Synthesis, structure and spectroscopic properties of the trinuclear cobalt(II) and nickel(II) complexes based on 2-hydroxynaphthaldehyde and bis(aminooxy)alkane. *Spectrochim. Acta A* **2015**, *135*, 342–350. [[CrossRef](#)] [[PubMed](#)]
68. Dong, X.Y.; Kang, Q.P.; Li, X.Y.; Ma, J.C.; Dong, W.K. Structurally characterized solvent-induced homotrinuclear cobalt(II) N<sub>2</sub>O<sub>2</sub>-donor bisoxime-type complexes. *Crystals* **2018**, *8*, 139. [[CrossRef](#)]
69. Dong, W.K.; Zheng, S.S.; Zhang, J.T.; Zhang, Y.; Sun, Y.X. Luminescent properties of heterotrinuclear 3d–4f complexes constructed from a naphthalenediol-based acyclic bis(salamo)-type ligand. *Spectrochim. Acta A* **2017**, *184*, 141–150. [[CrossRef](#)] [[PubMed](#)]
70. Bernstein, J.; Davis, R.E.; Shimoni, L.; Chang, N.L. Patterns in hydrogen bonding: Functionality and graph set analysis in crystals. *Angew. Chem. Int. Ed. Engl.* **1995**, *34*, 1555–1573. [[CrossRef](#)]
71. Kruszynski, R.; Sierański, T. Can stacking interactions exist beyond the commonly accepted limits? *Cryst. Growth Des.* **2016**, *16*, 587–595. [[CrossRef](#)]

72. Chen, L.; Dong, W.K.; Zhang, H.; Zhang, Y.; Sun, Y.X. Structural variation and luminescence properties of tri- and dinuclear Cu<sup>II</sup> and Zn<sup>II</sup> Complexes constructed from a naphthalenediol-based bis(Salamo)-type ligand. *Cryst. Growth Des.* **2017**, *17*, 3636–3648. [CrossRef]
73. Chai, L.Q.; Wang, G.; Sun, Y.X.; Dong, W.K.; Zhao, L.; Gao, X.H. Synthesis, crystal structure, and fluorescence of an unexpected dialkoxo-bridged dinuclear copper(II) complex with bis(salen)-type tetraoxime. *J. Coord. Chem.* **2012**, *65*, 1621–1631. [CrossRef]
74. Ma, J.C.; Dong, X.Y.; Dong, W.K.; Zhang, Y.; Zhu, L.C.; Zhang, J.T. An unexpected dinuclear Cu(II) complex with a bis(Salamo) chelating ligand: Synthesis, crystal structure, and photophysical properties. *J. Coord. Chem.* **2016**, *69*, 149–159. [CrossRef]
75. Gao, L.; Liu, C.; Wang, F.; Dong, W.K. Tetra-, Penta- and Hexa-Coordinated Transition Metal Complexes Constructed from Coumarin-Containing N<sub>2</sub>O<sub>2</sub> Ligand. *Crystals* **2018**, *8*, 77. [CrossRef]
76. Dong, W.K.; Shi, J.Y.; Zhong, J.K.; Tian, Y.Q.; Duan, J.G. Synthesis, crystal structure and infrared spectral analysis for a trinuclear nickel(II) cluster. *Chin. J. Inorg. Chem.* **2008**, *124*, 10–14.
77. Towatari, M.; Nishi, K.; Fujinami, T.; Matsumoto, N.; Sunatsuki, Y.; Kojima, M.; Mochida, N.; Ishida, T.; Re, N.; Mrozinski, J. Syntheses, structures, and magnetic properties of acetato- and diphenolato-bridged 3d–4f binuclear complexes [M(3-MeOsaltN)(MeOH)<sub>x</sub>(ac)Ln(hfac)<sub>2</sub>] (M = Zn<sup>II</sup>, Cu<sup>II</sup>, Ni<sup>II</sup>, Co<sup>II</sup>; Ln = La<sup>III</sup>, Gd<sup>III</sup>, Tb<sup>III</sup>, Dy<sup>III</sup>; 3-MeOsaltN = N,N'-bis(3-methoxy-2-oxybenzylidene)-1,3-propanediaminato; ac = acetato; hfac = hexafluoroacetylacetonato; x = 0 or 1). *Inorg. Chem.* **2013**, *52*, 6160–6178. [PubMed]
78. Mabbs, F.E.; Machin, D.J. *Magnetism and Transition Metal Complexes*; Chapman and Hall: London, UK, 1974; pp. 200–201.
79. Ginsberg, A.P.; Martin, R.L.; Sherwood, R.C. Magnetic exchange in transition metal complexes. IV. Linear trimeric bis(acetylacetonato)nickel(II). *Inorg. Chem.* **1968**, *7*, 932–936. [CrossRef]
80. Zhang, H.; Dong, W.K.; Zhang, Y.; Akogun, S.F. Naphthalenediol-based bis(Salamo)-type homo- and heterotrimeric cobalt(II) complexes: Syntheses, structures and magnetic properties. *Polyhedron* **2017**, *133*, 279–293. [CrossRef]



© 2018 by the authors. Licensee MDPI, Basel, Switzerland. This article is an open access article distributed under the terms and conditions of the Creative Commons Attribution (CC BY) license (<http://creativecommons.org/licenses/by/4.0/>).